International Journal of GEOMATE, June, 2020, Vol.18, Issue 70, pp. 252 - 280
ISSN: 2186-2982 (P), 2186-2990 (O), Japan, DOI: https://doi.org/10.21660/2020.70.68180
Geotechnique, Construction Materials and Environment

INTERGRATION REMOTE SENSING AND HYDROLOGIC, HYDROULIC MODELLING ON ASSESSMENT FLOOD RISK AND MITIGATION: AL-LITH CITY, KSA

*Ashraf Abd Elkarim[1], Mohsen M. Awawdeh [2], Haya M. Alogayell [3], and Seham S. S. Al-Alola [4]

[1] Research Center, Ministry of Housing, Riyadh, Saudi Arabia; [2] Social Studies Department, College of Arts, King Faisal University, Al-Ahsa'a, Saudi Arabia; [3] Geography Department, College of Arts, Princess Nourah bint Abdulrahman University, Riyadh, Saudi Arabia; [4] Geography Department, College of Arts, Princess Nourah bint Abdulrahman University, Riyadh, Saudi Arabia

*Corresponding Author, Received: 21 Jan. 2020, Revised: 20 Feb. 2020, Accepted: 27 Feb. 2020

ABSTRACT: This study aims to evaluate and identify potential floods in coastal areas with simple slopes of the Al-Lith valley basin, and to identify urban areas exposed to flooding with flood water in the coastal city of Al-Lith during the period between 1988-2019 as a model for the coastal city of Saudi Arabia, and designing strategies to mitigate the effects of floods and the establishment of a Department of Urban Planning Flood Risk. These are very important things for political and planning decision-makers, as the city suffers from repeated exposure to the risk of floods as a result of its occurrence directly below the Al-Lith valley basin. In order to reach these goals, the (Light Detection and Ranging, Lidar) data was analyzed to build and develop a two-dimensional model of the depth, speed and spread of water using a hydraulic model (Hydrologic Engineering Center-River Analysis System, HEC-RAS) to calculate the risk matrix of floods. Changes in Earth's use of the city of Al-Lith were monitored by analyzing consecutive satellite visualizations made by the American satellite Landsat in the years 1988, 2000, 2013, and 2019. The hydrological model (Hydrologic Engineering Center-Hydrologic Modelling System, HEC-HMS) was applied in calculating the floods hydrograph curve for the Al-Lith Valley basin during different return periods, and estimating the calculation of the amounts of flood water and flow rates depending on the (SCS Unit Hydrograph) method.

Keywords: Hydrological Modeling; Hydraulic Modeling; Risk Matrix; Urban Areas Prone to Flooding

1. INTRODUCTION

In recent years, many regions around the world have experienced unprecedented rainstorm events due to recent climate change. These events have created hazards that have led to different losses, including loss of property, economic losses, and loss of life. According to the Center for Research on the Epidemiology of Disasters (CRED) and the United Nations Office for Disaster Risk Reduction (UNISD) in the period between 1950–2017, most floods occurred during the last few decades, and about 2% occurred during the 1950s. and more than 60% of the total economic and human losses were concentrated between 1950 and 2017 in Asia and in Saudi Arabia. Thus, floods are one of the most frequent and devastating natural disasters [1].

The development of computers and related algorithms, the emergence of new sensors such as drones (Unmanned Aerial Vehicle (UAVs)), Global Positioning System (GPS), Lidar, Synthetic Aperture Radar (SAR), Image categorization, discovery of change, and artificial intelligence, help provide valuable spatial information to study hydrological and hydraulic processes in dry, data-scarce environments. This helped decision makers and planners to predict, monitor and assess flood risks.

Remote sensing also provided a real opportunity to reduce reliance on costly field surveys and barometric measurement stations used to measure flood characteristics, especially in remote areas and developing countries. It is one of the attractive alternatives that has received increasing attention during the past years in improving forecasts for hydrological and hydraulic models [2-4].

There is an emerging and ongoing opportunity to use the increasing data sets to improve hydrological forecasts and spatial modeling of flood risk, which provides the means for monitoring hydrological and hydraulic status variables, including length, temperature, soil moisture, water levels, evaporation, flood values, flood depth, speed, and spatial spread, which support the understanding of regional and global hydrological processes on a large scale in light of climate change and human activities.

Flood risk mapping and hazard analysis for any watershed or drainage basin engages with several factors, parameters, and criteria [5, 6]. Geographic information system (GIS) and remote sensing (RS) techniques have made significant contributions to natural hazard analysis [7, 8].

During the last few decades, researchers have

been involved in developing different methods and models for natural hazard mapping using RS and GIS techniques [9, 10]. The frequency ratio [11, 12], the analytical hierarchy process [13], fuzzy logic [14], logistic regression [15], artificial neural networks [16–18], weights-of-evidence [19], multi-criteria decision support systems [20, 21], and hydraulic modeling are fundamental tools for managing and mitigating flood risk [1, 22-27].

The first step to managing flood-exposed urban areas is preparing an indicator using the flood Hazard Index. Based on a survey of the literature reviews, flood hazard modelling over urban areas is shown to be one of the most widespread methods in the scientific and engineering communities. Flood hazard modelling depends on the hazard matrix, which relies on developing a 2D model that can compute the flood velocity, depth, and water spread using the hydraulic model (HEC-RAS) to assess the flood hazard. This method provides a 2D environment, which is vital in urban hazard modelling (Megan and others) [28].

One of the most prominent studies that used the hydraulic modeling method for the two-dimensional model was the study of Abdel Razek, Mohamed, and others [29] for flood hazard assessment in dry environmental urban areas. An important case study was performed at the campus medical university in Medina. This study adopted the HEC-RAS and its integration with the HEC-HMS and provided a map of the hazard-exposed areas.

Abd Elkarem, Ashraf Ahmed Ali, and others [1] applied a new approach to identify the exposed flood hazard urban areas of the city of Tabuk, offering a proposed mechanism for the city's protection that integrates both hydrological and hydrological modeling. The study developed by Hatem, Sharif, and others [30] focused on flood hazards in the urban watersheds in Riyadh city and was based on conducting simulation models for different urbanization scenarios. This study also determined flood hazard areas and affected roads through a simulation hydrological/hydraulic model and obtained a map of the vulnerable areas.

A pertinent study by Abd Elkarem, Ashraf, and others [31] This study aimed at measuring the impact of changes in land use morphology on the increase of flood risk through its application to the case of the Riyadh–Dammam train track in Saudi Arabia.

Megan et al. [28], Zahrani et al. [32], and Norhan et al. [33] developed simulated models of water inflow relationships and precipitation using an HEC-HMS model in the dry environment of the Aqiq valley, Madinah, Saudi Arabia. Sampath et al. [34] determined the relationships between precipitation and water runoff using the HEC-HMS model in Sri Lanka's tropical watersheds, and Meling et al. [35] used the HEC-HMS model to simulate the water runoff in semi-arid zones in the northwest of China. Locharya and Mansouri [36] used the HEC-HMS model with frequent storms to simulate a runoff hydrograph in a small urban watershed in Northeast Algeria. Khalil and others used the HEC-HMS model [37] and the Muskingum–Cunge approach to compute the lost outflow of secondary watersheds by using GIS-based methods for the Al-Lith valley in Saudi Arabia.

There has been a significant focus recently [38-40] on the use of highly accurate digital altitude data for flood risk modeling where (Lidar) provides accurate data, especially in flat areas with simple slopes where flood plains disappear and become difficult to identify on topographic maps, space imagery, and traditional low-resolution elevation models. Establishing more accurate studies regarding the identification of potential floods in coastal areas with simple slopes is something that needs more studies and research, especially in areas with scarce data and in developing countries. The coastal city of Al-Lith is one of the Saudi coastal cities that need such studies.

Two main aspects are creating serious national problems for the valley floodplains: urban expansions and continuous changes in the land use patterns of Saudi cities. Because these plains represent the main zones of the agricultural, urban, service, and economic activities of Saudi cities, their potential severity and dangerousness to the country is increased. Thus, floodplains are considered a direct threat to the lives, services, and economic activities of the population.

The vast majority of Saudi cities are located in valleys or within the low-lying areas positioned at the bottoms of valleys, as excessive infringement on the valleys and changing water paths have contributed to increasing the destructive effects of floods on the urban areas in the alluvial fans and along the valleys.

Al-Lith city is one of the coastal cities on the eastern Red sea coast (KSA), which is exposed to floods and frequent hazards due to its position at the bottom of a major valley, the Al-Lith Valley. The physical nature and conditions of the cities located in coastal zones along the Red Sea are mostly similar; these cities include Jeddah, Thule, Zahban, Yanbu, Amlaj, and Rabigh and are similar to Al-Lith, since all are exposed to torrential flood events. The last event that flooded Al-Lith city was on 25 November 2018, the floodwaters had a recorded height of more than 1.7 meters in some areas of the city. This caused more than 21 individuals to drown, obliterated more than 487 houses, destroyed the infrastructure, and caused a complete collapsed of all facilities and institutions of the city (fig. 1).

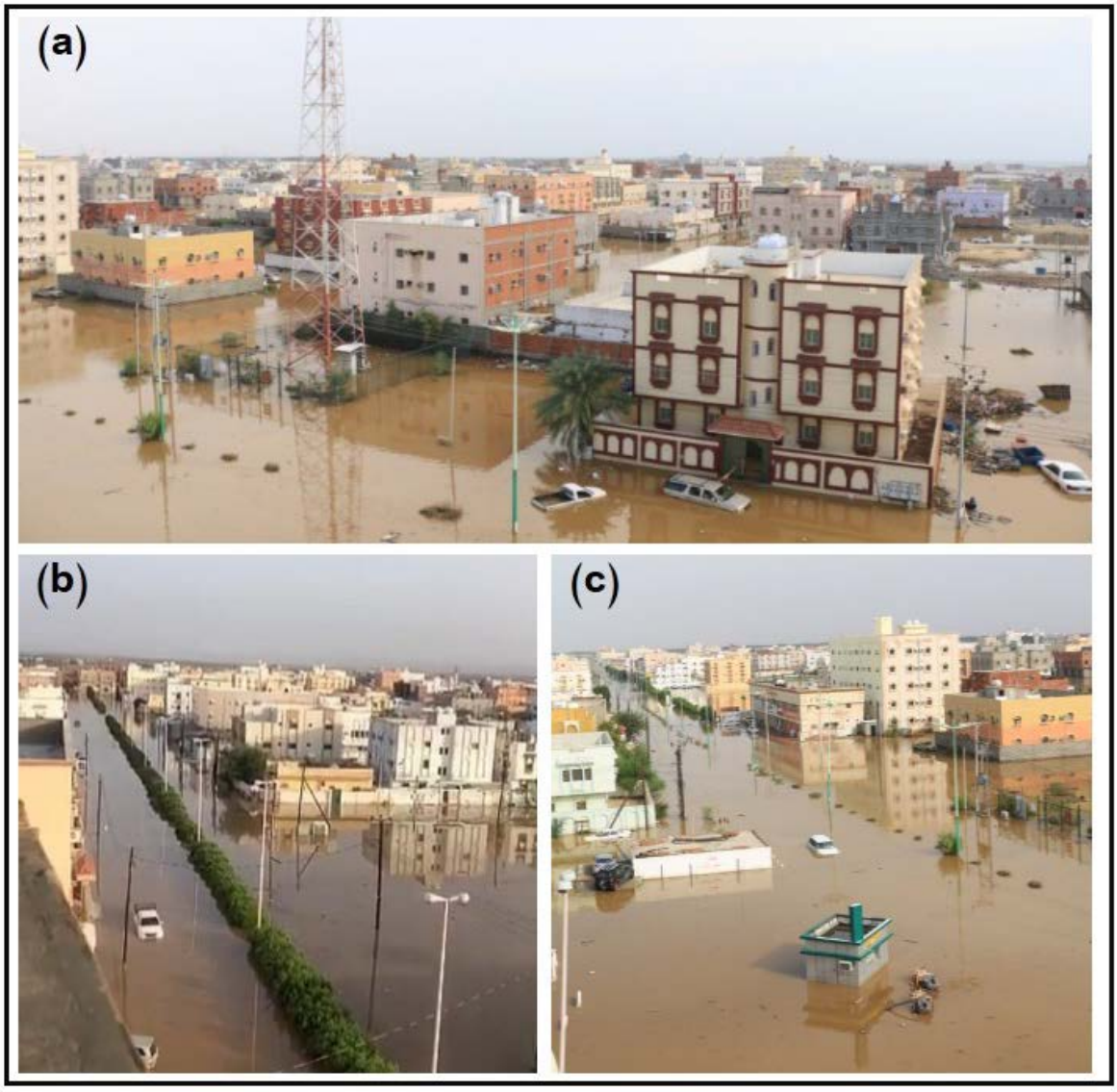

Fig.1 Floods of Al-Lith city in 25 November 2018. Picture (A) shows the water flooding Al-Lith city, and pictures (B, C) illustrate that the flood water increased its level by more than a meter in the streets of the city

This study aims to manage the flood risks for the urban environment of the city of Al-Lith by defining the path of the Al-Lith valley and its flood plain and borders near the urban cluster of the city of Al-Lith. The difficulty in determining these factors from topographic maps, aerial photos, digital elevations, as well as the difficulty in determining the depth, speed, and flood movement of the Al-Lith valley in a one-dimensional model necessitates the creation of a two-dimensional model using the hydraulic modeling program HEC-RAS.

We also evaluate the abilities of the existing floodwater drainage facilities represented by ferries, bridges, and bridges constructed under the Jazan–Jeddah road to pass the peak flows to the valley; monitor urban changes in the land use map during the period of 1988–2019 for the city of Al-Lith to determine the directions and axes of urban expansion, as well as the future of urban growth and its relationship to risks; develop a map of areas subject to flooding with flood water based on the construction of a two-dimensional model (HEC-RAS) program for simulating the spread, depth, and speed of flood waters in light of the continued adoption of urban plans (without taking into account the paths of the valleys and reefs in addition to the continuous backfilling work by parents and planners); and developing suitable proposals, alternatives, and scenarios to mitigate the risks of the Wadi Al-Lith flood, which all aim to reduce the damage to life, property, and infrastructure. This study uses an innovative approach for the KSA based on RS, GIS, the watershed modeling system (WMS), the Hydrological modeling (HEC-HMS), and the Hydraulic modeling (HEC-RAS).

Alternative protective measures are proposed in the study area to help mitigate the impact of floods on Al-Lith City.

2. STUDY AREA

Al-Lith city is located in the Mecca zone, on the Jeddah-Jizan highway as a part of the Tuhama region in the western coastal zone of Saudi Arabia. This city extends between the latitudes of 20°6"24.28' and 20°10"40.83' North and the longitudes of 40°14"55.43' and 40°20"27.4' East (see fig. 2, 3). Al-Lith city is situated about 180 kilometers from Mecca and 190 kilometers from the southern boundary of Jeddah. Jeddah city is positioned not far from its west northern boundary, and it shares a boundary with Al Qunfudhah, which is located in the south eastern section, as the Red see relies on the south and south western boundary. The east and east northern boundaries reflect the desert environments of the Mecca zone. Al-Lith city is estimated to be 7040 Ha and has a population of 159186 with a total of about 16245 families (the general authority of statistics, 2017).

The discharge basin of the Al-Lith valley, which impacts the area of study, lies between the latitudes of 20°7"23.57' and 21°6"51.07' North and the longitudes of 40°11"39.67' and 40°48"39.42'; the basin extends for 144 kilometers in length, with a total area of 3120.8 square kilometers. The basin begins in Ablea Mountain at 2012 meters above sea level and ends 13 meters above sea level, as it is fed by different Sub-valleys, such as Algoawf, Bathan, Kanfer, Faleh, Alkhessr, and Tasbeh.

3. METHODOLGY AND DATA PROCESSING

Figure 4 shows a flow chart of the methodology, which consists of four basic components that can be illustrated as follows:

3.1. Monitoring the Land Use Changes in the Al-Lith City during the Period From 1988 to 2019

To identify and monitor the land use changes of the Al-Lith City during the period from 1998 to 2019, the ERDAS IMAGINE 2016 program was used. The process for monitoring these changes has four basic phases [31].

The first stage entails the uploading of satellite images. Every ten years, images were taken by the United States Geological Survey Site (USGS) to monitor the changes that occurred in Al-Lith City. The first image was taken in 1988, and the second was taken in 1998 from the sensor (Thematic Mapper, TM), mounted on the American satellite Landsat 4–5; the third was taken in 2013 from the sensor (Operational Land Imager, OLI), mounted on the American satellite Landsat 4–5; and the fourth image was taken in 2019 from the mobile OLI sensor, mounted on the Landsat 8 satellite (Table 1), The second stage involves spectral enhancement. The latter stage was performed to increase spectral accuracy and reduce spectral interference through the raster menu, including the spectral icon and the principal component option.

The third stage handles the process of supervised classification, and the fourth stage entails accuracy assessment. By using the error matrix for the maximum likelihood method and applying the kappa coefficient (which was also performed by the error matrix), the accuracy was rated using the main menu raster. Classification, including supervised classification, included an accuracy assessment option.

From the edit menu in the accuracy assessment window, random points were added and used to test the accuracy of the classification (number of random sample points = 100 points). Random sample points with a value (zero) that expressed unclassified areas were deleted and unclassified by the order criteria using the equation Class = 0.

Table 1 The characteristics of the satellite images used in monitoring the urban changes of Al-Lith City during the period from 1988 to 2019

Date of Capture	1988	2000	2013	2019
Path	169	169	169	169
Row	46	46	46	46
Satellite	Landsat 4–5		Landsat 8	
Spatial Accuracy	30	30	30	30
Sensor Type	TM	TM	OLI	OLI
Bands	7	7	11	11

Then, choosing the select and delete selection, all unclassified samples were deleted, and the sample points were shown on the satellite images by selecting the satellite image window of the view menu and then selecting viewer. Then, the points were shown on the image by selecting “show all” from the view list.

To calculate the accuracy of the classification after entering the ranks of the report list and the accuracy report, a final report was generated with all the details, which showed the total accuracy of the classification and the classification accuracy of each phenomenon (Table 2).

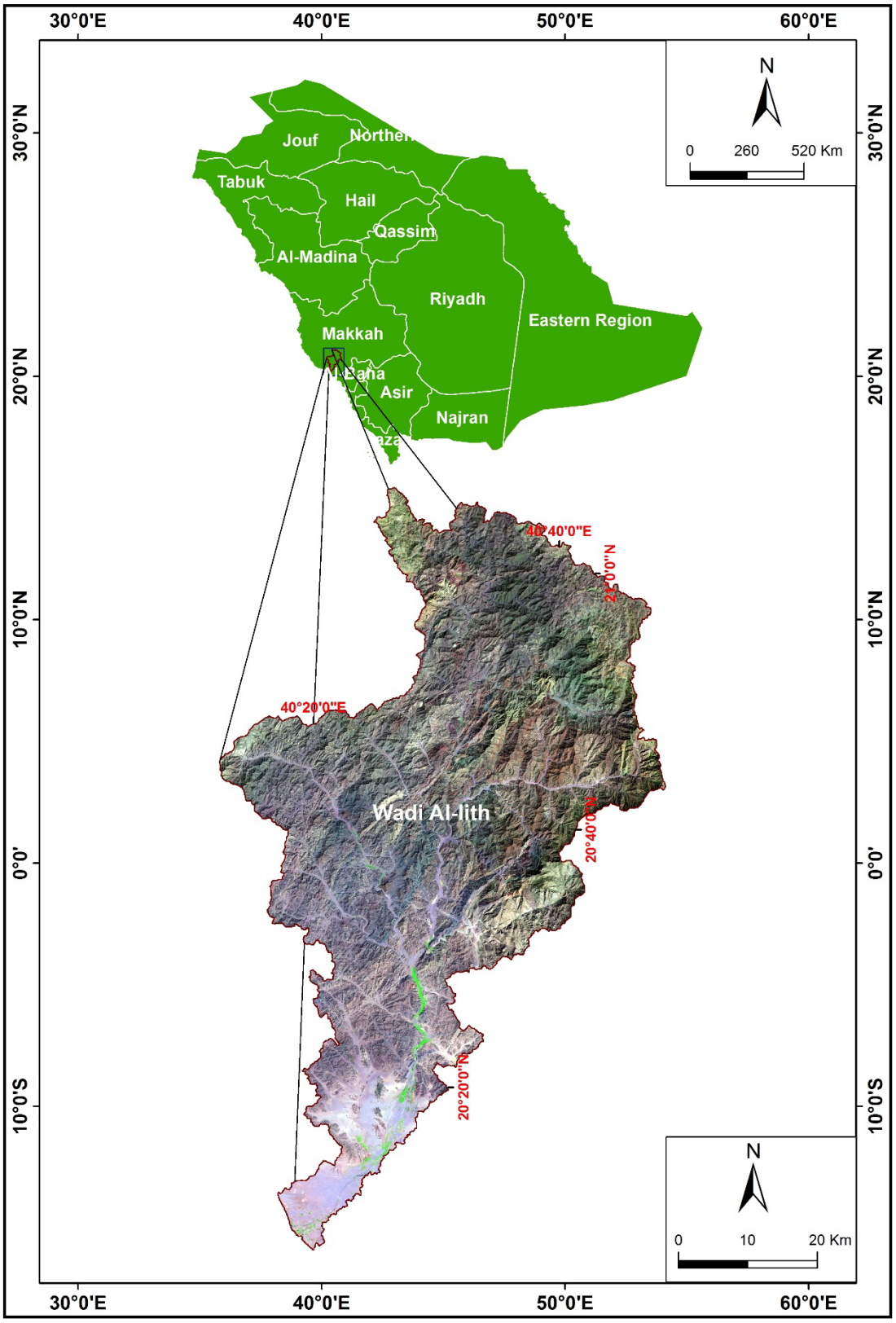

Fig. 2 The Study Area of Wadi Al-lith

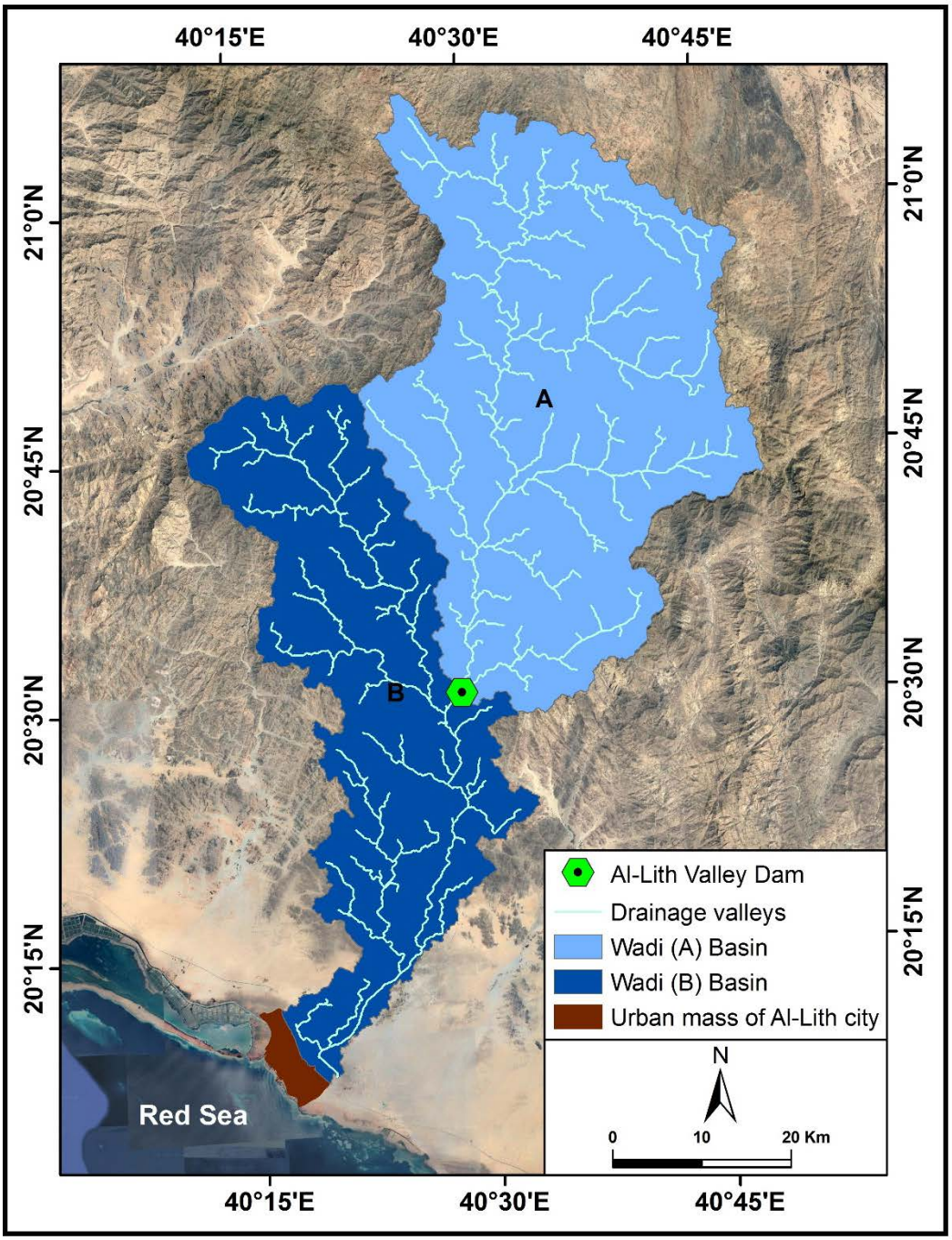

Fig. 3 Discharging basins affecting Al-Lith city in 2019

Table 2 Classification accuracy of satellite images in monitoring the urban changes of Al-Lith City during the period from 1988 to 2019

Image Date	Classification			
	Type	Method	Overall	Kappa
1988	Supervised Classification	Maximum Likelihood	100%	1
2000	Supervised Classification	Maximum Likelihood	95%	0.92
2013	Supervised Classification	Maximum Likelihood	96%	0.89
2019	Supervised Classification	Maximum Likelihood	92%	0.9

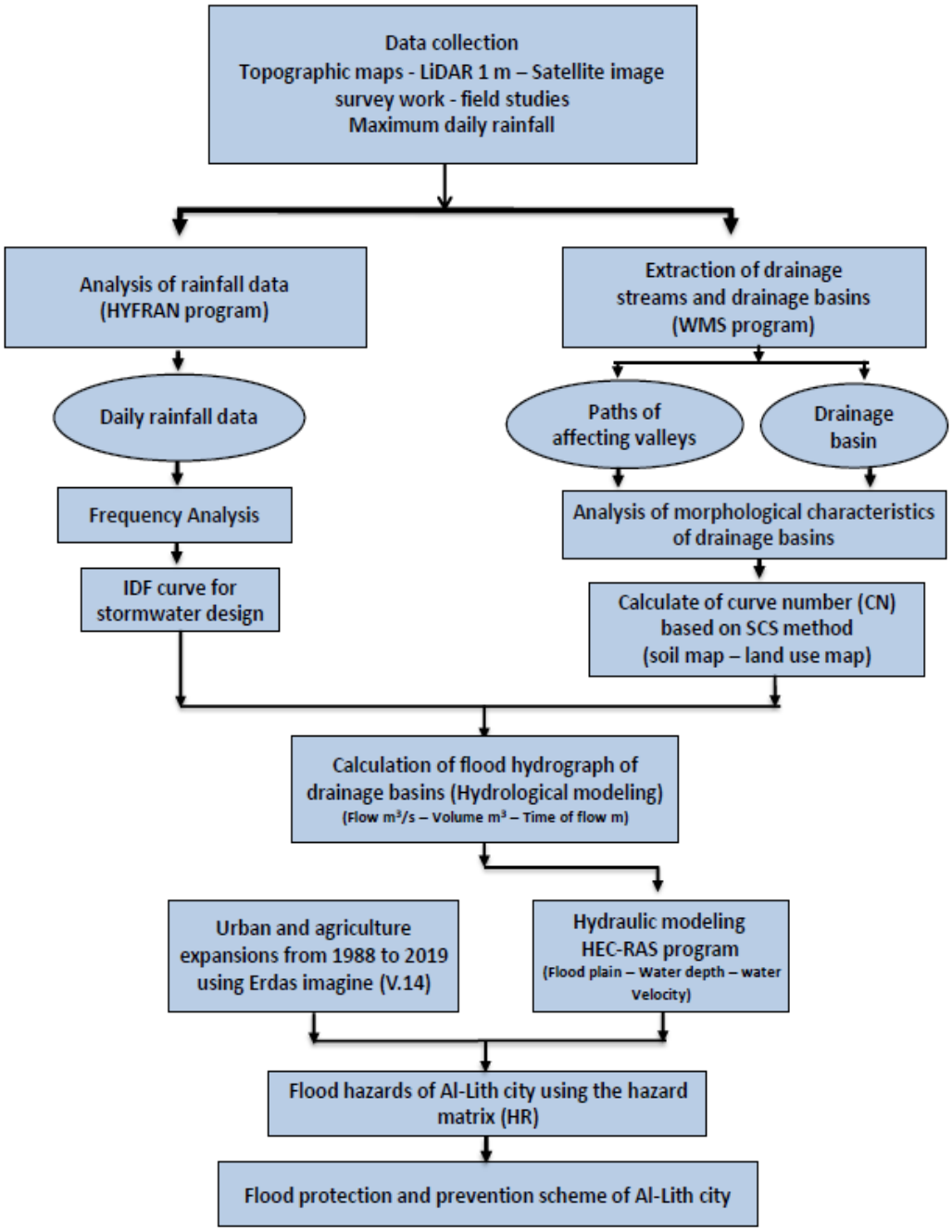

Fig. 4 The methodology for studying the urban environmental management of flood hazards in Al-Lith city in 2019

The total image classification accuracy in 1988 was about 100% of the total samples used in the test. The total classification accuracy of the equation is calculated by Eq. (1).

$$\boldsymbol{Overall} = \frac{\sum_{i=l}^{K} xil}{N} \quad \textbf{(1)}$$

Where N is the total number of samples, and $\sum_{i=l}^{K} xil$ is the total correct samples for all classified phenomena.

The Kappa coefficient was also about 1, as calculated from Eq. (2).

$$\boldsymbol{Kappa} = \frac{N \sum_{i=l}^{K} xil - \sum_{i=l}^{K} (xi+ \times x+i)}{N^2 - \sum_{i=l}^{K} (xi+ \times x+i)} \quad \textbf{(2)}$$

Where N is the total number of samples, $\sum_{i=l}^{K} xil$

is the total correct samples for all classified phenomena, and $\sum_{i=l}^{K}(xi + \times x + i)$ is the total product determined by multiplying the total number of samples and the number of correct samples per phenomenon [41].

For the image rating of 2000, the accuracy of the satellite image classification was about 95% of the total samples used in the test (i.e., 5% of the total samples differed when evaluating accuracy), and the kappa coefficient was about 0.92. For 2013, the accuracy of the satellite image classification was about 96% of the total samples used in the test (i.e., 4% of the total samples differed when evaluating accuracy), and the kappa coefficient was about 0.89. For 2019, the accuracy of the satellite image classification was about 92% of the total samples used in the test (i.e., 8% of the total samples differed when evaluating accuracy, and the kappa coefficient was about 0.9).

3.2. Hydrological Modeling

The HEC-HMS [25] has been applied to calculate the hydrograph curves in multiple ways—for both simple and complex drainage basins and by natural or artificial methods. HEC-HMS is one of the programs globally used in the field of hydrology and was developed by the American Army Organization. Using a 24 h storm design, a SCS TYPE II distribution was used, and the SCS method was used to calculate the delay and concentration times for different frequency times of 100, 50, 20, and 10 years. The output of the hydrological model used in our study was deduced to infer the hydrograph of the water's drainage basins.

The network of the valleys of the wadi Al-Lith basin was identified and extracted using several different sources, the most important of which is the high-LiDAR model of m. The sources are from the website of King Abdulaziz City of Science and Technology, Institute of Space Research. Topographic maps at a scale of 1:50,000, with 13 plates, were taken from the Saudi Geological Survey Authority; a modern satellite image from the Landsat 8/OLI was derived from the US Geological Survey Site (USGS); and a modern geological map at a scale of 1:250,000, with 6 plates, was derived from the Saudi Arabian Geological Survey.

It was necessary to use mathematical equations that represented the rain loss or link runoff and total rainfall to calculate the curve number and the greatest drainage (m^3/s). The Kirpich equation [42] was used in the calculation of the time of concentration, which is the time needed for rainwater falling on the surface of the basin to gather until it reaches the point where the flow is calculated by Eq. (3):

$$t_c = 0.0195\left(\frac{L^{0.77}}{S^{0.385}}\right) \quad (3)$$

Where tc is the time of concentration (min), L is the maximum flow distance (m), and S is the maximum flow distance slope (%).

The delay time was calculated using the SCS method, which is the time between the occurrence of a unit of rain and the occurrence of a unit of water runoff Eq. (4):

$$T_{LAG} = \frac{L^{0.8}[Sr+1]^{0.7}}{1900\sqrt{Y}} \quad (4)$$

Where T_{LAG} is the lag time (hour), Sr is the maximum effort for soil moisture (maximum retention) calculated from the curve number (cm), and Y is the basin slope (%).

The depth of rain or direct flooding in the basin was calculated to infer the total flooding at the actual rain value (Eq. (5)–(7)). The amount of water in the area before the occurrence of a flood, such as the water resulting from infiltration and rainwater found on plants, was also estimated using Eq. (5). Eq. (4) can be simplified, as illustrated in Eq. (7).

$$Q = (P - Ia)2/(P - Ia + S) \quad (5)$$

$$Ia = 0.2Sr \quad (6)$$

$$Q = (P - 0.2Sr)2/(P + 0.8Sr) \quad (7)$$

Where Q is the direct flooding (cm); P is the rainfall for different return periods (cm), Sr is the maximum effort for soil moisture, and Ia is the amount of water before the occurrence of a flood, such as filtration and suspended rain on plants.

The maximum soil moisture was then calculated, where CN represents the curve number in the Soil Conservation Services (SCS) method. This coefficient depends on land uses and the nature of the soil [43] determined using Eq. (8).

$$S = (1000/CN) - 10 \quad (8)$$

The maximum drainage (m^3/s) of each basin was calculated for different return periods using Eq. (9).

$$qp = \frac{0.208AQ}{Tp} \quad (9)$$

where qp is the peak discharge (m^3/s), A is the basin area (km^2), Tp is the time to peak (hour), and Q is the direct runoff (mm).

The greatest drainage time was calculated using Equation (10):

$$Tp = \frac{\Delta t}{2} + T_{LAG} \quad (10)$$

3.3. Hydraulic Modelling

Two-dimensional hydraulic modelling was carried out using HEC-RAS, version 5.0.4, from the Center for Hydrological Engineers. This program can calculate the movement of sediments and chemical pollutants in the current, evaluate channels and passes, and assess distal stalactites. This program is used to map the spread of floods and calculate the risk of floods in threatened places. The applications of this program are used to calculate the rates of degradation and aggradation resulting from the flood water currents, and the two-dimensional modelling from HEC-RAS [31] was employed to calculate the speed, depth, and spread of the Wadi Al-Lith flood. The construction of the two-dimensional hydraulic model was achieved using HEC-RAS with four stages: (a) Correction, or the addition of engineering data for transverse sections and hydraulic structures; (b) the peak flow of the data input; (c) the general definition of the model plan (the engineering data files and flow are set based on the results of previous hydrological modelling and the high 1 m LiDAR model and (d) the implementation and verification of hydraulic calculations.

3.4. Hazard Classification Using the Hazard Matrix (HR)

The hazard matrix shows the spatial dimension of the expected floods in different scenarios that may be present under both qualitative and quantitative approaches. A hazard assessment is undertaken to determine the certain expected hazard in a particular future period, as well as its effected area and impacts. This approach is more distinctive for its applicability to urban areas. Water depth maps were developed, as well as maps for flood velocity and flood intensity. (Table 3) clarifies how the hazard levels due to the HEC-RAS the cross section must be established and inserted to run this model, as well as the inflow rate at the valley's starting point (m^3/s).

Using the Energy conservation equation, the computation of water depth and velocity is applicable [44], since this model has obtained accurate and effective results in related flood studies [45,46]. Using hazard assessment (HR), (Fig. 5) illustrates the classifications of hazards affecting human beings, and (table 4) shows a hazard classification map based on hazard assessment (HR), which depends on the water depth and velocity. The risk equation is measured in Eq. (11).

$$\mathbf{HR = d(v + 0.5) + DF} \quad \mathbf{(11)}$$

Where HR is the risk rate, d is the flood water depth (m), v is the flood velocity (m/w), and DF is a coefficient that takes sediments into account. The value of DF is assumed to be 5.0 for depths lower than 25.0 m and 0.1 for depths greater than or equal to 25.0 m

Table 3 Flood intensity levels

levels of severe flood	Maximum water depth (m)		Water maximum outcomes (h) with the highest velocity V (m^2/S)
high	h> 1.5 m	or	v h >1.5 m^2/s
Moderate	0.54 m < h< 1.5 m	or	0.5 <vh< 1.5 m^2/s
Low	0.1 m < h< 0.5 m	and	0.1 m^2/s <vh< 0.5 m^2/s

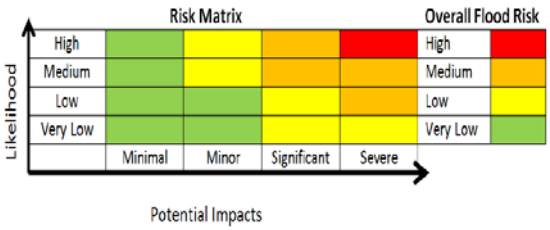

Fig. 5 Classification of hazards to humans using hazard assessment (HR)

Table 4 Hazard classification using hazard assessment (HR)

Risk rate	Risk categories impacted the Human	Color symbol
Less than 0.75	Very low risk	
0.75: 1.25	Risk for some ages, including children and elderly	
1.25: 2.00	Risk for majority, including entire population	
More than 2:00	Risk for all, including emergency cases	

The study methodology and data processing are through six main steps, as follows:

3.5. Precipitation Quantity Analysis of The Different Regression Periods and Determination of The IDF Curves

The accurate determination of the dropped precipitation over the watershed is considered to be

one of the main factors necessary to compute the volume of the flood water as this value reflects the correct foundation of the water's statistical operations and the expected frequent floods.

According to the documented records of both the Ministry of Water and Electricity and the General Authority of Meteorology and Environmental Protection, three Meteorological stations control the Al-Lith valley: Al-Lith (J108), Al-shifa (TA109), and Belkarn (TA233).

All stations have recorded data that reflect different periods of time (43, 54, and 36 years, respectively). The water inflow depth was calculated for different frequent inflows for 2, 5, 10, 20, 50, and 100 years using Hyfran [47]. Moreover, different statistical patterns were implemented, including Normal, Log-Normal, Log-Pearson Type III, Pearson Type III, Gumbel, and Exponential. These patterns demonstrated that the ideal method to compute the inflow of the data collected from the three metrological stations is the "Log-Normal" method, as shown in (Figs. 6,7,8,9, 10 and table 5).

Table 5 Rainfall water inflow depth for different times at the Metrological Stations of Al-Lith (J108), Al-shifa (TA109), and Belkarn (TA233)

Frequent Periods	Al-Lith (J108)	Al-shifa (TA109)	Belkarn (TA233)
2	20.8	39.8	38.8
3	31.5	50.2	51.8
5	46.8	62.8	68.3
10	71.5	79.8	91.8
20	101	97.2	117
25	112	103	126
50	150	121	154
100	195	141	185

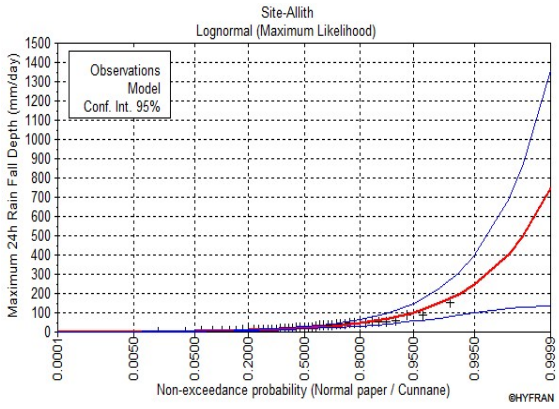

Fig. 6 Probability distribution curve of the station data for the Al-Lith station (J108) using the Log normal method

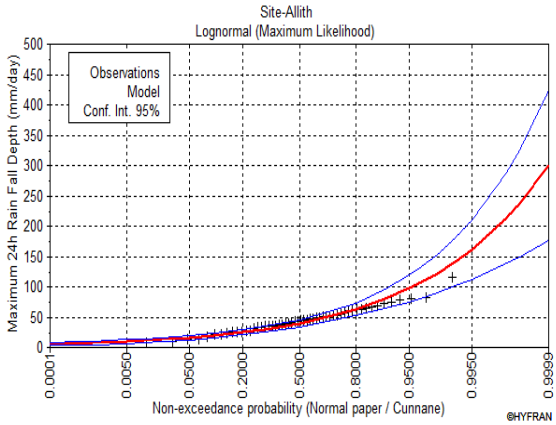

Fig. 7 Probability distribution curve of the station data for the Al-Shefah station (TA109) using the Log normal method.

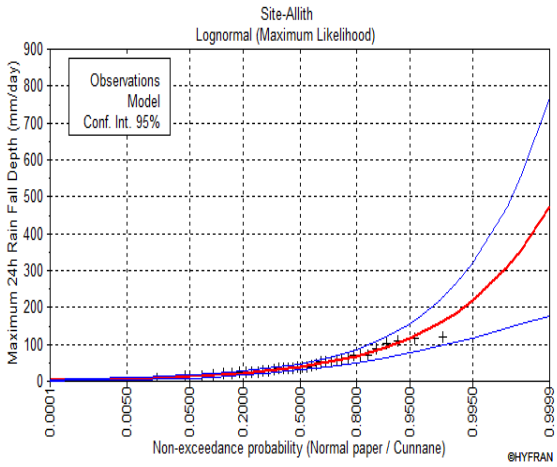

Fig. 8 Probability distribution curve of the station data for Belkarn station (TA233) using the Log normal method.

3.6 Digitizing and Extracting Valleys and Basins of the Basin of the Al-Lith Valley

The digitization and extraction operations of the valleys and basins in the watershed modeling system (WMS) run via the drainage module, which is listed in the DEM menu, which is the main menu for such a function. This operation is accomplished by computing the flow direction and accumulation. Then, the program creates TOPAZ to clarify the water's inflow directions. The Al-Lith valley is shown to be highly affected by Al-Lith city, according to the obtained comparison between the extracted data from the given LiDAR (with a 1 m resolution), as well as the topographic maps of 1:50000 and the satellite images. The Al-Lith valley was divided into main two sub-basins (A, B) for the attendance of the Al-Lith Dam, which was built to store water (see fig. 11).

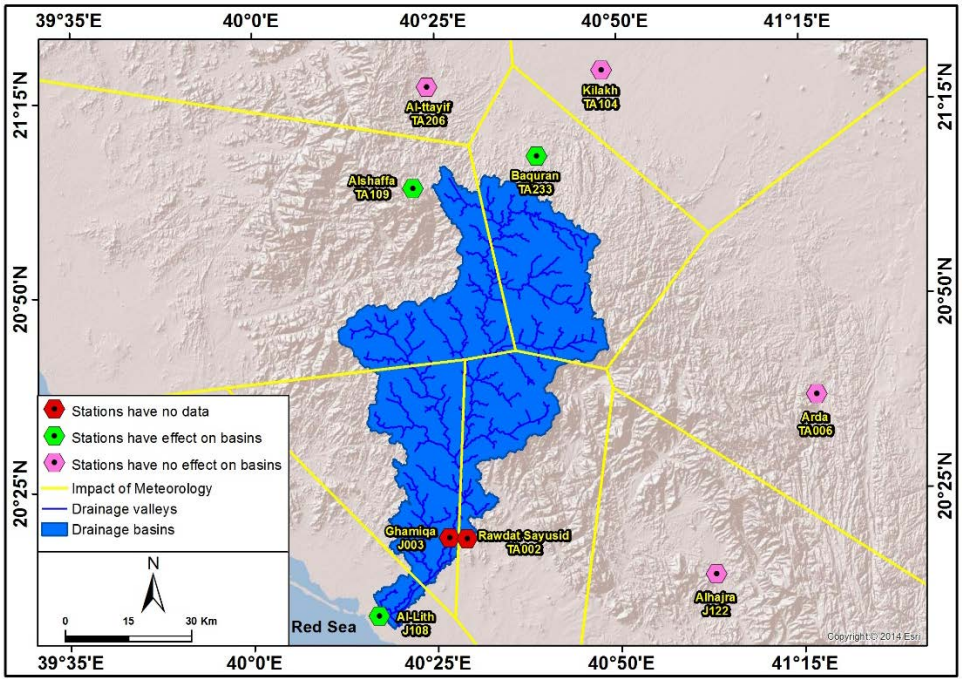

Fig. 9 Sites of the surrounding rainfall measurement stations present in the basin of the Al-Lith valley, using the Tyson polygons method, in 2019

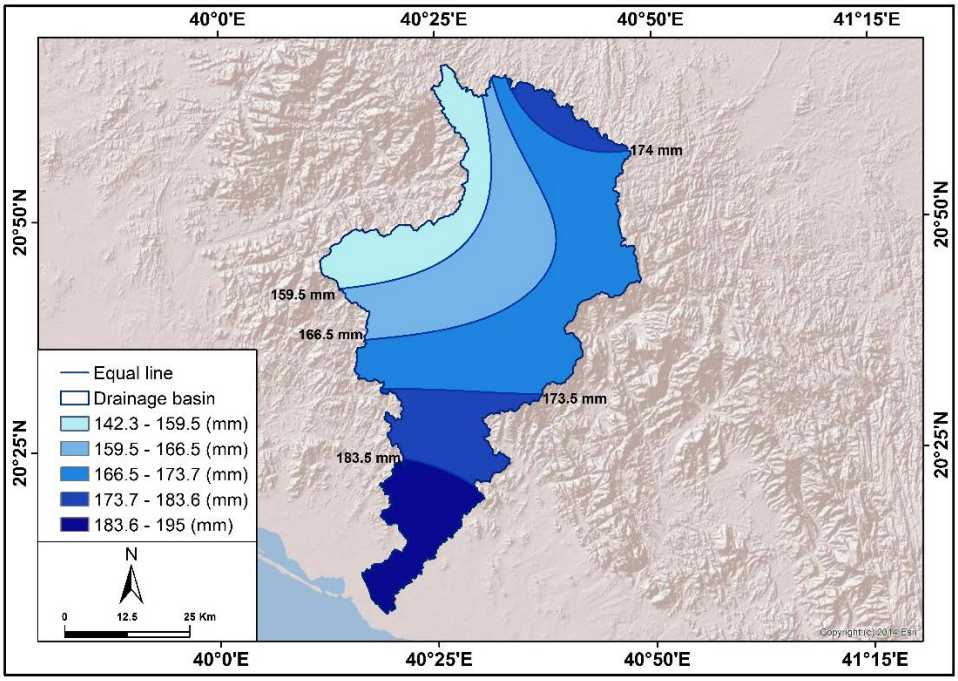

Fig. 10 The annual rainfall ISO lines of the basin of the Al-Lith valley effecting Al-Lith city in 2019.

3.7. Morphological Characteristics of the Basin of the Al-Lith Valley

The Al-Lith basin is highly affected by the city of Al-Lith, as the basin's area is almost 3120.8 Km^2 and extends with a longitudinal distance of 144.3 Km.

The Al-Lith basin is divided into two main discharging sub-basins (A,B), similar to the Al-Lith dam, which stores flood water where it is separated. The water inflow sourced from the northern direction (Basin A) will be excluded from the water stored recently by dam.

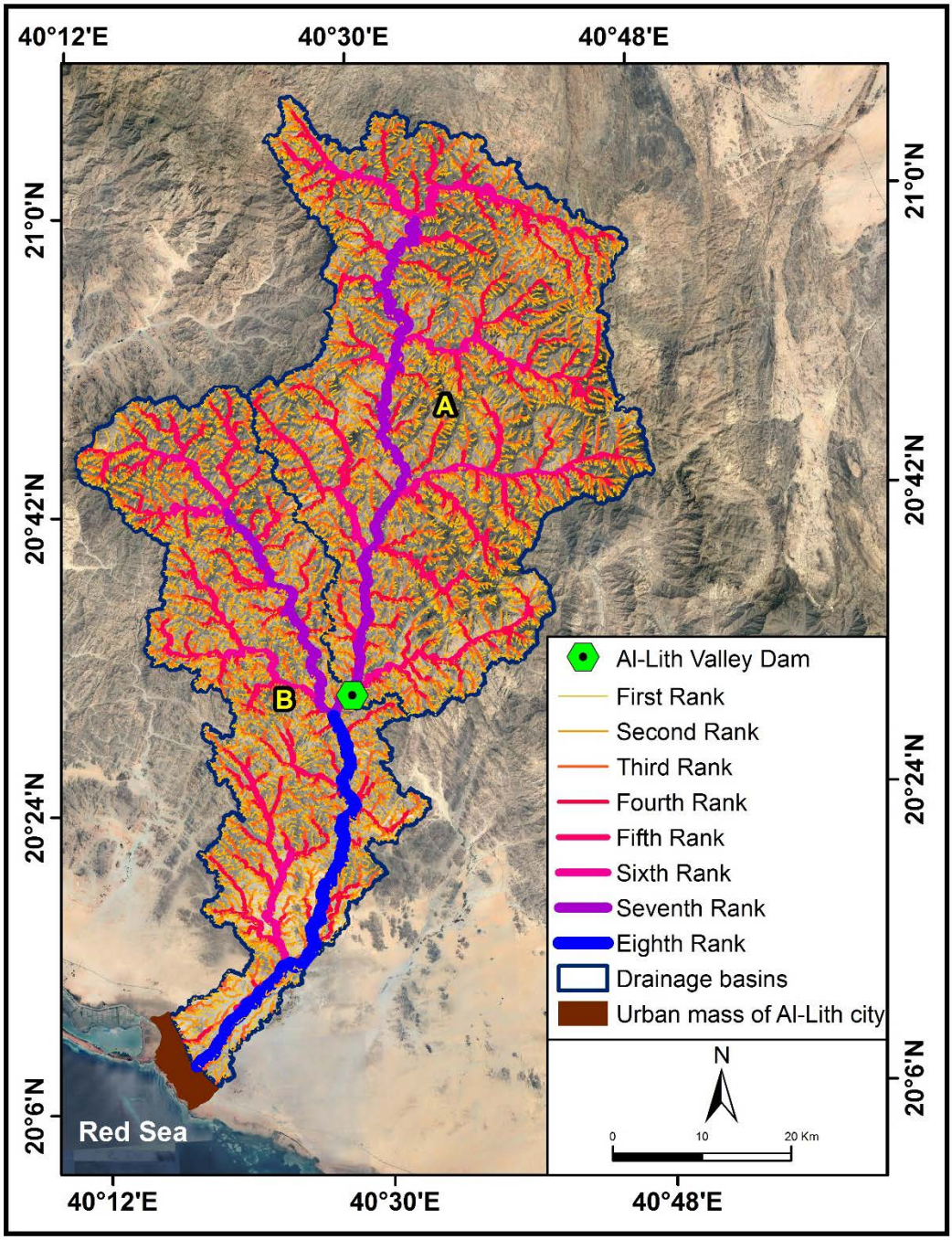

Fig. 11 ranking map of the valleys in the Basin of the Al-Lith Valley in 2019

The basin (A) extends about 67022.1 m, and its watershed area reaches 1890.2 Km^2, as its slope is almost 0.3702 m/m. Basin (A) is considered a transferred flood water basin, as it transfers the rainfall from the north to south direction, whereas basin (B) is about 77240.5 m in longitude, with an area of 1230.6 Km^2, its slop reaches 0.2118 m/m, as it also transfers the flood water (see table (6)).

Table 6 Morphometric characteristics of the water discharging basins affecting the Al-Lith site, 2019

Basin Name	A	B
Area (Km^2)	1890.2	1230.6
Length (m)	67022.1	77240.5
Basin slope (m/m)	0.3702	0.2118
Average level (m)	1156.6	369.1
Delay time (Hr.)	5.5	7.2
Concentration time (Hr.)	9.2	12.0

3.8. Definition of The Hydraulic Group of the Basin of the Al-Lith Valley

The two main critical factors to compute the curve number (CN) are the determination of the soil's hydrological group and the land use, since the CN value is based on both variables. The (SCS) method has determined four soil hydraulic groups [48], as per the velocity rate of the water transmitted through it. These four groups are A, B, C, and D, each of which has its own inflow runoff characteristics. The water discharging basins of the Al-Lith valley can be divided into these four groups, since group A occupies an area of 144.95 Km^2, thereby illustrating highly permeable soil.

On the other hand, group (B) presents clay soil with an area of 881.55 Km^2, as it includes deposits of valleys, volcanic rocks, and a composition of Basan with Schist–Biotite rocks. Group (C) shows an area of 858.22 Km^2, as it presents a mud soil structure. Group (C) includes various rocks, such as diorite, annular granite, gabro, granite form, bentlite, nouman, and monzogranite formations, while group (D) involves low transmission mud soil with an area of 1236.08 Km^2, containing basalt, quartz, tunaalite, granite, garnodorite, orthogenize rocks and Al-Khaserah formations. (Figs. 12, 13).

3.9. The Land use of Basin of Al-Lith Valley

The land use was obtained by using the satellite image classification of Landsat 8/OLI through the Erdas Imagine software, and the land use layer was defined by the water modeling system (WMS) program. This process was started by inserting the land use layer after selecting the layers according to new coverage using GIS data and selecting add share file data. There are three main sets of land use in the Al-Lith basins. The first set is the desert areas, with an area of 3090.16 Km^2, while the second set includes urban areas, with an area of 5.23 Km^2 of the total discharging basin area of the Al-Lith valley. Finally, the third set shows the agricultural yields, with an estimated area of 25.41 Km^2 (see fig. 14).

3.10 Computation of The Curve Number of the Basin of the Al-Lith Valley

To compute the extra rainfall quantities, it is necessary to use mathematical formulas to calculate the rainfall losses or the rainfall linked between the runoff inflow and the total precipitation. The present author used one of the most popular methods to estimate the rainfall water losses through leakages to the underground: the Curve Number method. This method is based on three factors: the condition of the per-moisture soil, the land cover, and the soil hydraulic group, whose value ranged between 0 and 100, reflecting the water's response to the land cover formed in discharging basins. This method presents the solid area of the land's surface, whose value trends toward 100 as the surface becomes less solid [42].

4. RESULT AND DISCUSSION

4.1 Results of the Hydraulic Modeling of the Basin of the Al-Lith Valley

The mathematical model was implemented using a designed storm duration of 24 hours. By using the SCS II type pattern, as well as the SCS approach, this model was also used to compute the delay and concentration periods. All these approaches are used for different repeated times (e.g., 2, 3, 5, 10, 20, 25, 50, and 100 years), as the results of hydrologic model (HEC-HMS outputs) are obtained to catch the flood water hydrographs for the different discharging basins. The hydrograph analysis shows that the flood volume varies from one discharging basin to another, since the discharging basin (A) is ranked first, with a flood volume average reaching about 127,152,606.6 m^3. This volume is followed by discharging basin (B), with a flood water volume beyond 81,059,586.3 m^3, which is used for the reference period of 100 years, as shown in (table 7) and (figs. 15,16).

4.2 Estimation of the Maximum Flood Inflow of the Basin of the Al-Lith Valley

The values of the maximum flood inflow vary in the basin affecting the Al-Lith valley. This variation impacts the area of study due to the different precipitation volume over the total area of each basin. The flood volume discharge differs from one basin to another; accordingly, the inflow maximum volumes at the project site range between 1,852.52 and 3,599.62 m^3/s. The discharging basin (A) recorded the largest inflow volume, since the maximum inflow reached 3,599.62 m^3/s, followed by basin (B), with an average inflow reaching 1,852.52 m^3/s in the reference period of 100 years, as shown in table (table 7) and (figs. 15,16).

4.3 Estimated Latency for Maximum Flood Inflow of the Basin of the Al-Lith Valley

The hydrograph analysis of the main flood discharging basins shows that the maximum inflow period ranged between 1080 minutes for basin (A) and 1185 minutes for basin (B) for the reference period of 100 years, as shown in (table 7) and (figs. 15,16).

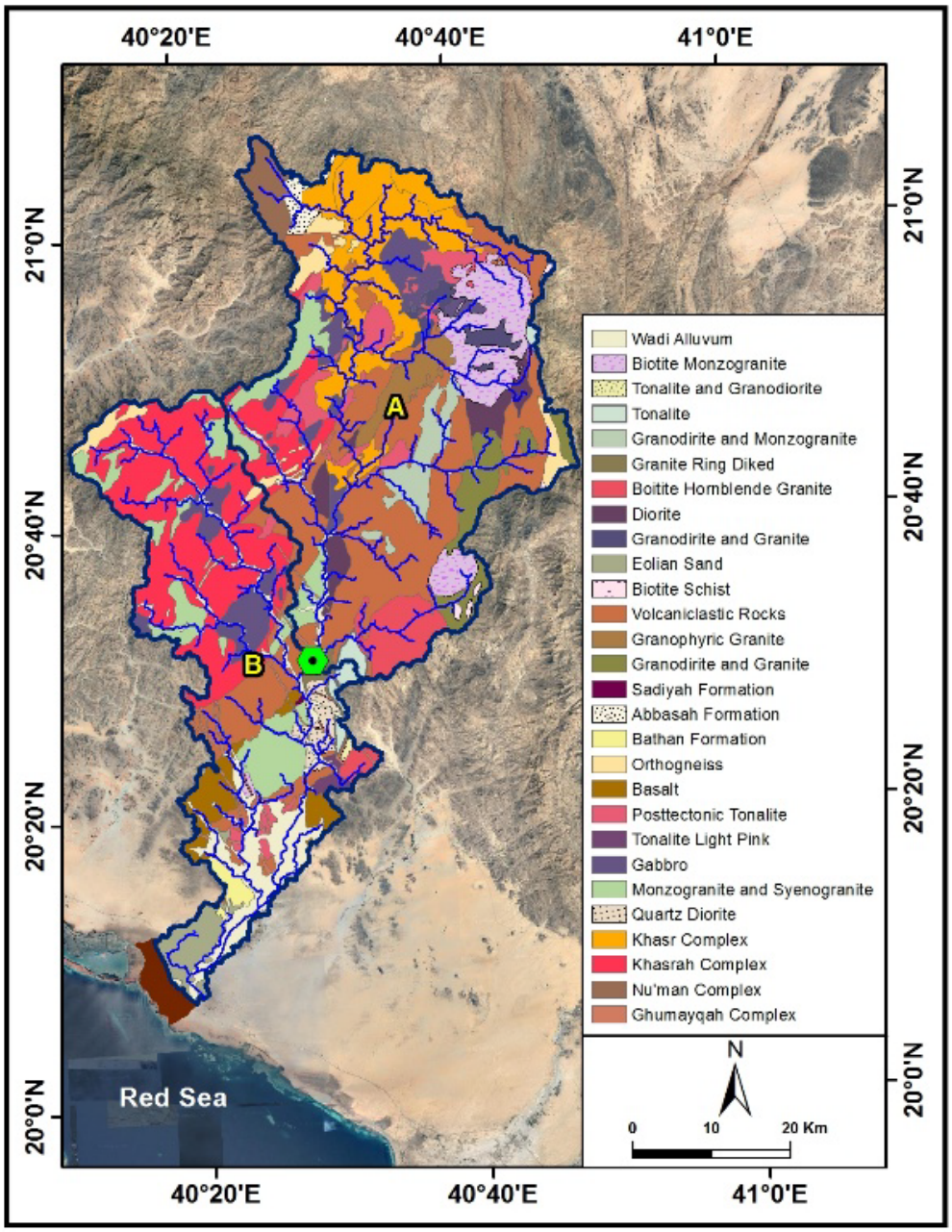

Fig. 12 Geological map of the soil of the basin of Al Lith valley effected Al Lith city in 2019

Table 7 Flood water characteristics for the discharging basin of the Al-Lith valley for different frequent periods

Basin name	A			B		
	Peak discharge (m^3\s)	Flood volume (m^3)	Time of peak (min)	Peak discharge (m^3\s)	Flood volume (m^3)	Time of peak (min)
5	809.80	30324629.2	1095	410.41	18882337	1215
10	1610.31	58204634.9	1080	820.45	36685632.2	1200
20	2599.92	92447507.2	1080	1331.22	58684748	1200
25	2928.71	103843836.5	1080	1502.31	66025368.9	1185
50	3358.25	118757722.5	1080	1726.4	75642066.4	1185
100	3599.62	127152606.6	1080	1852.52	81059586.3	1185

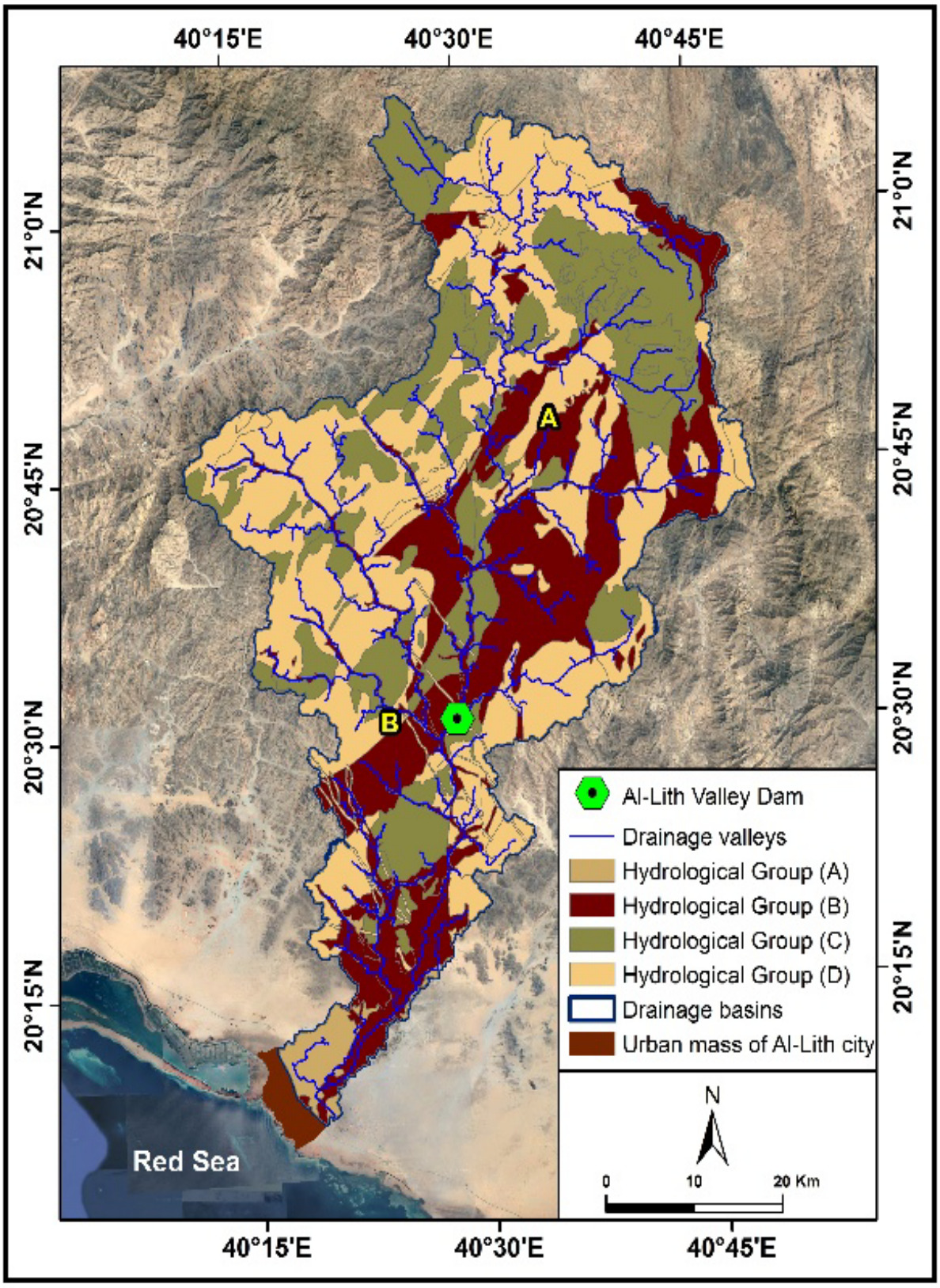

Fig. 13 Hydrological soil group of the basin of Al Lith valley effected Al Lith city in 2019

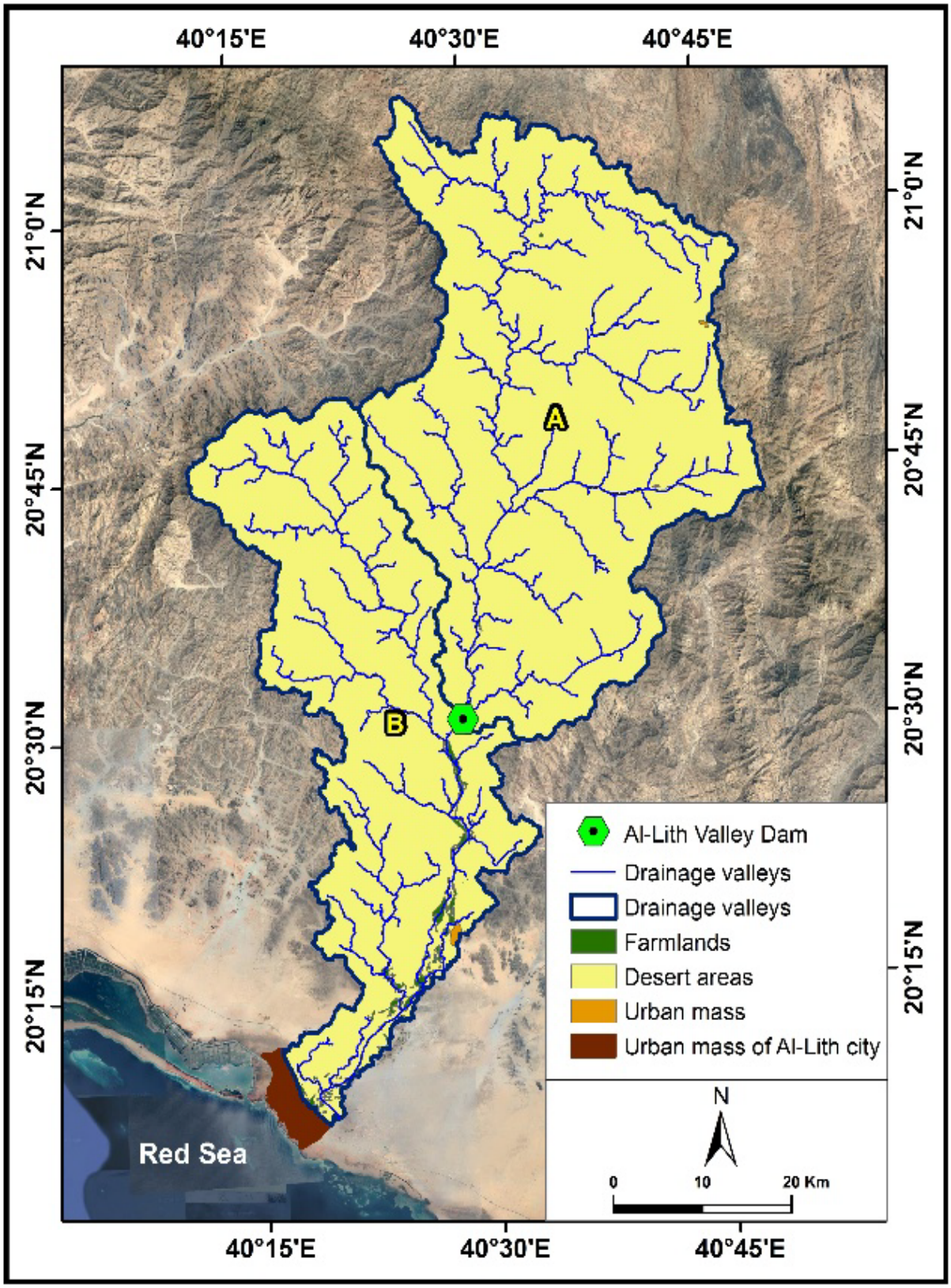

Fig. 14 Land use effects of the basin of the Al-Lith valley on Al-Lith city in 2019

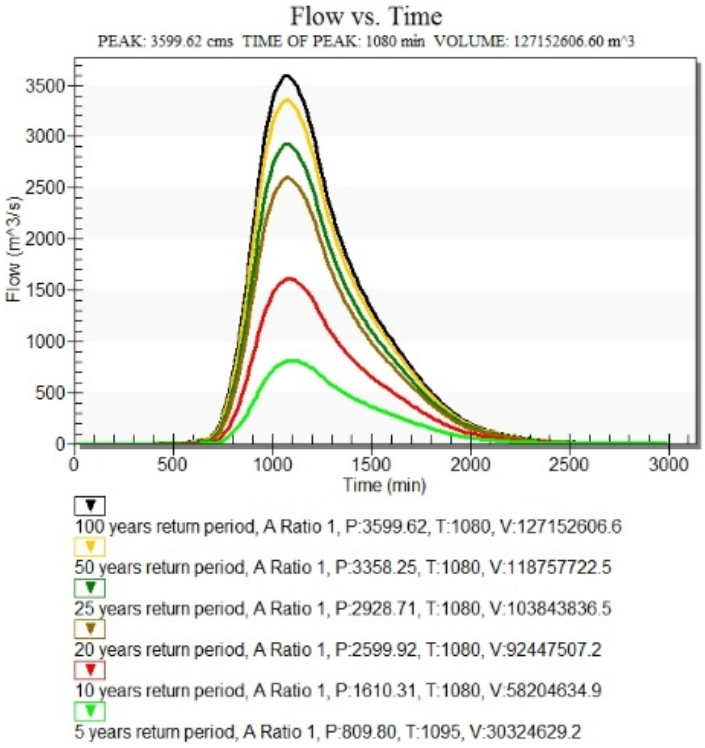

Fig. 15 The hydrograph flood inflow of basin (A) for various regression periods (5, 10, 20, 25, 50, and 100 years) in 2019

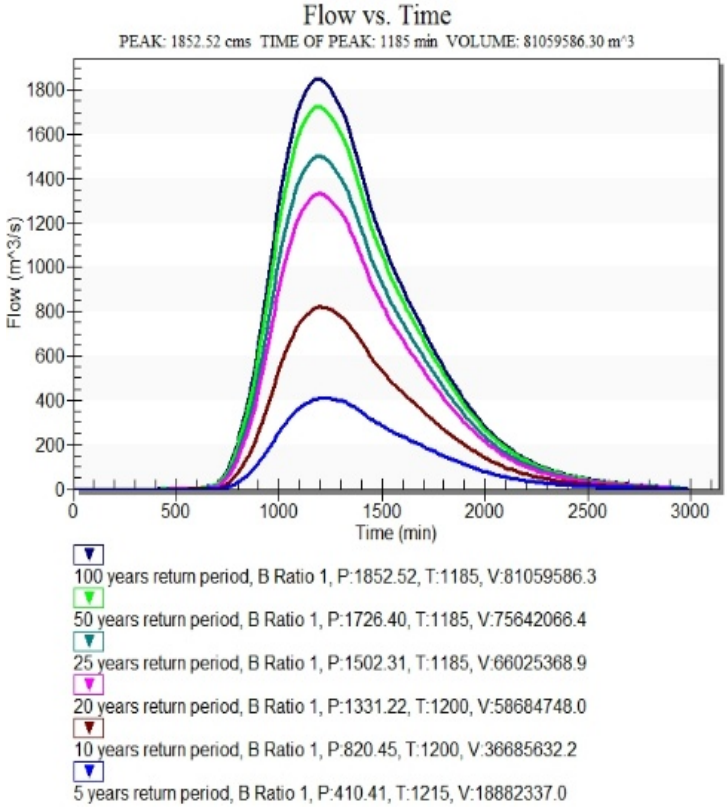

Fig. 16 The hydrograph flood inflow of basin (B) for various regression periods (5, 10, 20, 25, 50, and 100 years) in 2019

4.4. The Flood Characteristics of the Basin of the Al-Lith Valley and Verification of the Flood Risk Model of the Basin of the Al-Lith Valley

Table 8 The Flood characteristics of the Basin of the Al-Lith Valley as depth (m), velocity (m/s), Hazards (m^3/s)

Severity	0–1.5 (low)	1.5–3.5 (Moderate)	More than 3.5 (high)	Total
Characteristics of the Al-Lith valley (depth "m")	11.44	7.15	10.01	28.6
%	40	25	35	100
Characteristics of the Al-Lith valley (velocity "m/s")	11.44	11.44	5.72	28.6
%	40	40	20	100
Characteristics of the Al-Lith valley (Hazard "m^3/s")	10.01	14.3	4.29	28.6
%	35	50	15	100

The different research instruments, including the field study, analysis conducted on the given information in (table 8), and (figs. 17, 18) aimed to determine the flood scenarios that occurred on 25 November 2018.

The obtained results demonstrate that the simulation results tend to accurately reflect reality. The moderate hazard category (1.5–3.5 m^3/s) is dominated by 50% and constitutes about 14.3 Km^2 of the urban areas that are subject to flooding in the Al-Lith Valley. These urban areas are located in the urban plans in the north of Al-Lith city, particularly in the housing schemes, as well as concentrated in the southern parts next to the secondary school in Al-Lith.

The high classified hazard category (above 3.5) constitutes almost 15%, with an area of about 10.01 Km^2 of the total exposed flood area in the Al-Lith valley and is concentrated in the northern parts of the housing schemes and the planned land grant areas. Finally, the low hazard category (0–1.5 m^3/s) controls a share of 35% and forms about 4.29 Km^2 of the flood-exposed urban areas. These areas are intensively located in the southern parts of the city. Accordingly, Al-Lith City has expanded urbanely in most areas exposed to flood hazards that require decisive intervention by those responsible for managing and planning the urbanized environment in the city to establish a proper mechanisim to mitigate flood hazards in the Al-Lith valley.

Historical flooding events were used and satellite images were employed to verify the latest floods in the region on 25 November 2018. We also used this study to verify the validity of the models. Considering all the estimates of experts and comparing them with the results of the model, this study could not use results similar to those for neighboring basins, where the study area and most of the dry valleys suffer from a lack of measurements for their torrents and floods.

The checkpoints in study area indicate that the water level rose by 3.5–4 m, the water speed was 2–2.5 m/s, and estimates of the peak discharge ranged between 950.41–1760.80 m^3/s. These points were obtained from the database of the Saudi Geological Survey of the Al-Lith Valley flood. Most of the results obtained from this verification indicate the reliability of the hydrological and hydraulic model built in this study based on hydraulic and hydrological modelling.

4.5. Exposed Flooding Urban Areas at Al-Lith City

Several studies have been carried out to evaluate the impact of land use changes on runoff amounts [49–53]. Also, many authors have acknowledged the fact that increasing urban activities in flood plain areas will increase peak discharge, decrease the time to peak, and increase runoff volume [54–58]. A better understanding and evaluation of land use changes that have a direct impact on watershed hydrologic processes has become crucial for the planning, management, and sustainable development of the watershed [59–62]. These studies used land use changes to predict the potential for floods and to mitigate flood hazards, Recently, remote sensing and GIS have been used as powerful and effective tools to determine land use changes, map flood inundation, and to assess flood risk using satellite images with the help of hydrologic and hydraulic models [63–67].

In the current study, ArcGIS 10.2 was used to extract quantitative information based on the results of the hydrologic (WMS) and hydraulic (HEC-RAS) modeling, as well as the interpretation of the RS images completed with Erdas Imagine based on the current sections of urban expansion and how they have been impacted by flash flood hazards at different times.

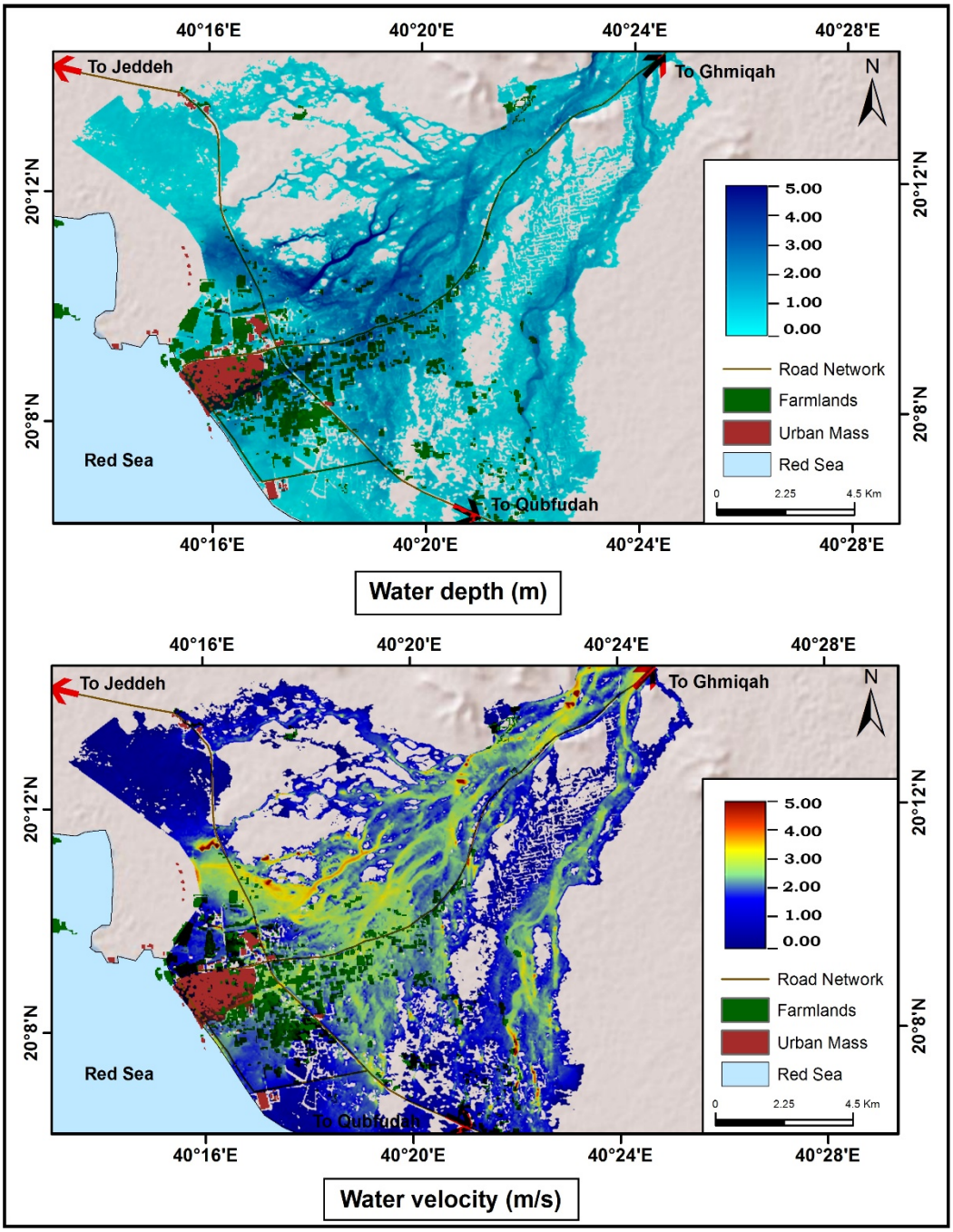

Fig. 17 Map of the flood water velocity and depth of the Basin of the Al-Lith Valley affecting Al-Lith city in 2019

Four stages were analyzed to understand the urban changes and the sub-basins impacted by urban distributions.

The data analysis showed that Al-Lith city experienced prosperity in developing its urban areas, as more than 3.4 times its total area was added in 1988 to increase its urban area. The city's urban area was then developed from 129.6 ha in 1998 to about 434.52 ha in 2018. The total urban growth reached almost 304.9 ha; this growth area was expanded over thirty years, with an average annual growth rate of 3.98% and 10 ha.The period between 2000 and 2013 was the highest recorded period for urban growth during the historical record of the city. The annual urban growth rate peaked at 7.15% when recording the maximum average of the annual increase during the same period, as almost 17 ha were added to 4.51% out of the total urban increase in the city. One of the most important increased urban areas was the housing schemes and the planned land grant areas, which are commonly exposed to flood immersion.

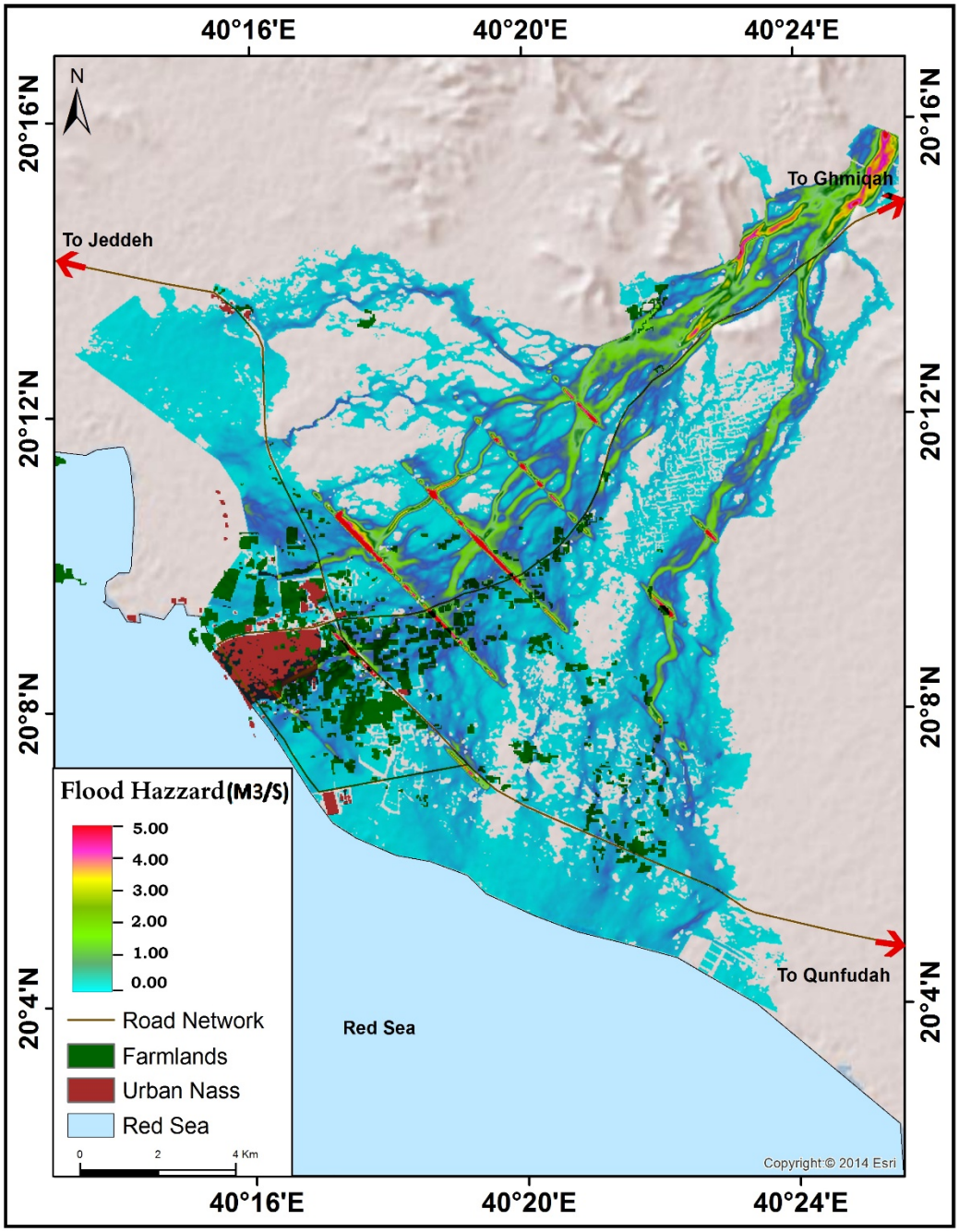

Fig. 18 Areas exposed to flooding and hazard severity of Al-Lith city in 2019

The other increases in the surrounding areas of Al-Lith City were the agriculture yields over thirty years between 1988 and 2018. This increased area attained 1265.0 ha with a 12.26% growth rate and an increased average of 41 ha.

The agriculture yields expanded by 36.05 times in 1988 and again developed from 36.09 ha in 1998 to 1301.04 ha in 2018. Clearly, the expanded urban and agriculture yields did not consider the flood hazards of the Al-Lith valley (see Table (9) and figs. 19, 20, 21).

The urban areas exposed to flood hazards are concentrated in the northwestern districts and in the new western urban schemes. These areas include about 70% of the total flood hazard exposed areas containing about 159 thousand people, according to the population survey of 2017. These areas are shared with almost 35% of the city's residences [37]. This areas include the Al eskan, Alfaysaleya, and Alshefa districts, while the south districts involve almost 30% of the flood hazard exposed areas and about 65% of the city's total residences, including the Koshan, Zedan and King Fahd districts.

Fig. 19 Part of the Floods of Al-Lith city in 25 November 2018. Picture (A) shows the water runoff of the Al-Lith valley near the international Jizan–Jeddah Highway, and picture (B) illustrates the exposure of the international Jizan–Jeddah Highway to the flooding of the Al-Lith valley.

Table 9 Urban growth phases of Al-Lith city between 1988 and 2019

Growth period	Area (ha)	Total increase		From year 1988 %	Average of annual increase (ha)	Annual growth rate %	1988–2019 Change rate %
		ha	%				
1988	129.6						
2000	153.36	23.8	5.47%	18.33%	2	1.41%	18.33%
2013	376.56	223.2	51.37%	172.22%	17	7.15%	145.54%
2019	434.52	58.0	13.34%	44.74%	10	2.41%	15.39%
1988–2019		304.9	70.17%	235.28%	10	3.98%	70.17%

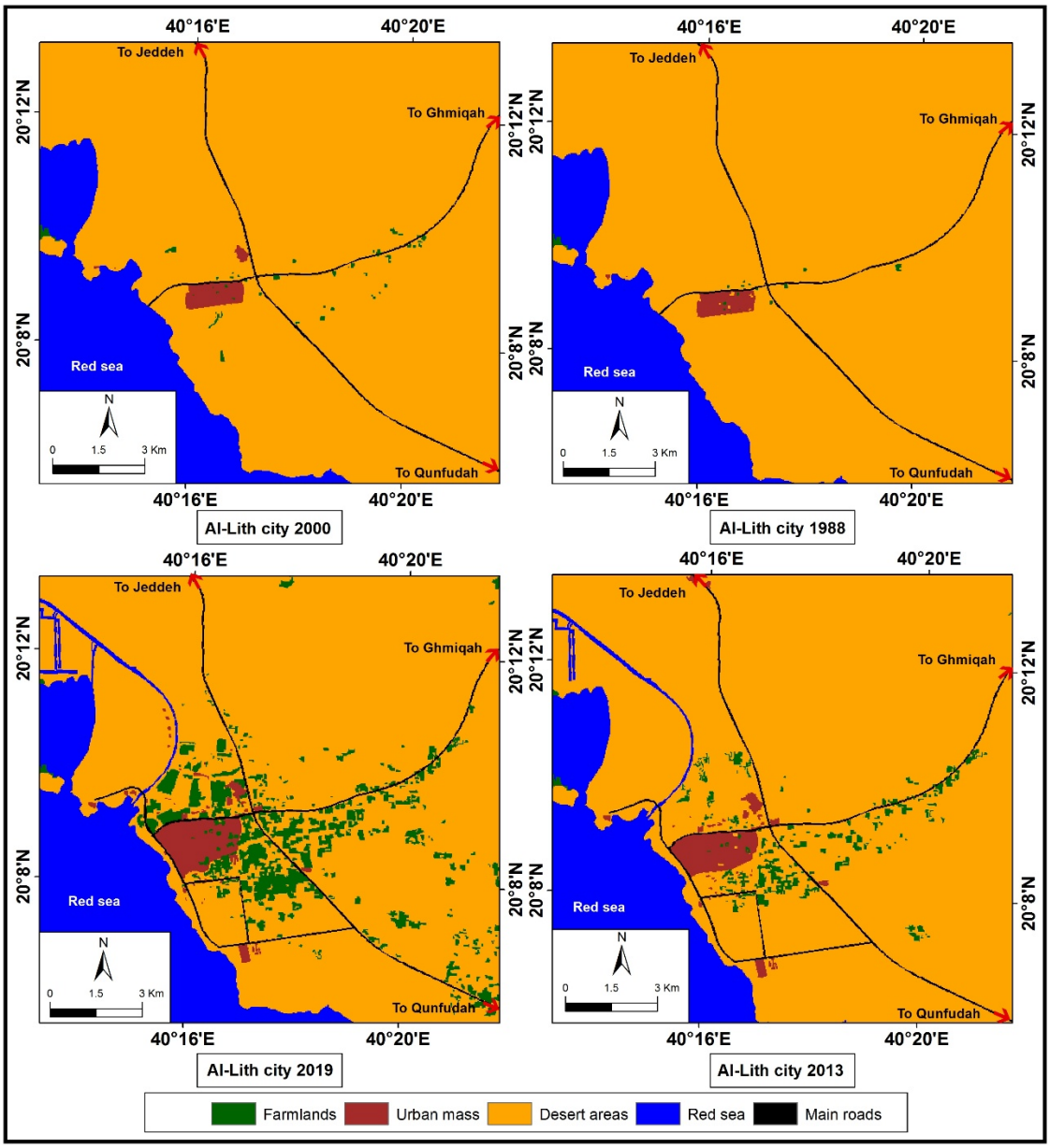

Fig. 20 Urban and agriculture changes of Al-Lith city during 1988–2019

The study's outcomes indicated that Al-Lith city, with its current boundaries, is totally exposed to immersion if the Al-Lith valley were to become flooded. The total immersed area reached 28.6 Km^2 and thus belongs to the high hazard category (More than 3.5 m^3\S), a share of 15%.

5.6. The proposed mechanism to mitigate the impact of floods on Al-Lith City

The recommendations of this study give priority to flood hazard prevention and infrastructure protection plans by preserving the existence of flood water discharging buildings, such as bridges, with continued maintenance. This must be accomplished with an engineering intervention (fig. 22) by implementing Canal (1), which collects and adjusts the flood water inflow from basin (B) to help it enter the urban area using the maximum inflow quantity of the frequency period of 100 years, which is estimated to be almost 1852.2 m^3/s. Canal (1) is recommended to discharge the flood water that flows in the valley beginning in the east and ending in the west. The canal bottom's width is 300 meters, with the following dimensions: a depth of 1.6 meters and a length of 9.5 Kilometers.

The study also recommends implementing Canal (2), which collects and adjusts the floodwater inflow coming from the east of the Al-Lith valley. This canal is located in the north of the Al-Lith valley and prevents the flood inflow to the urban mass using the maximum inflow of 100 years as the frequency period, estimated at about 599.6 m^3/s.

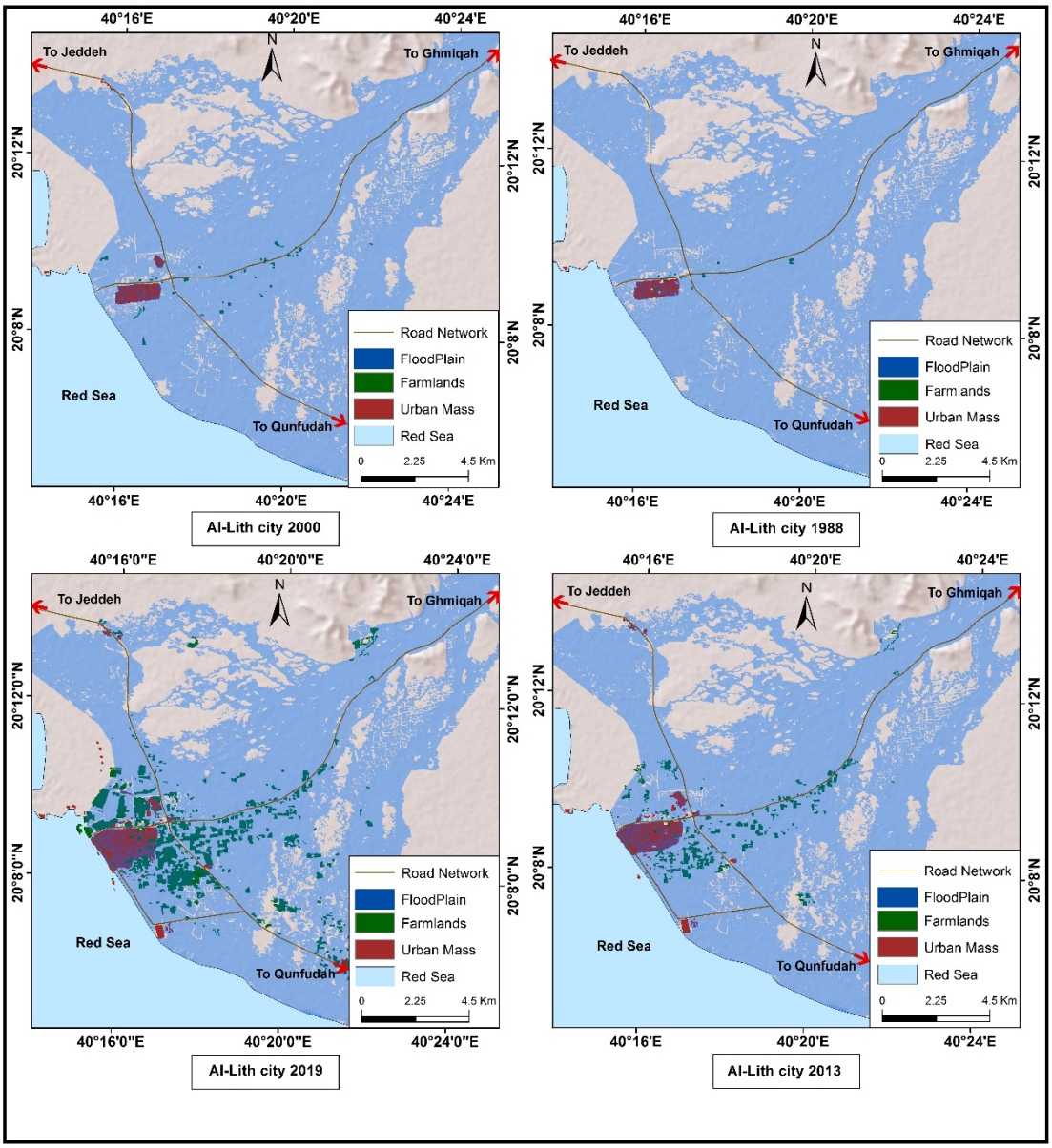

Fig. 21 The relationship between urban expansion and increasing the flood hazards of Al-Lith city during 1988–2019

Canal (2) is recommended to be implemented to discharge the valley flood water, starting from the eastern side and progressing through the city to reach the Robyan stream and then exiting to the Red sea. This canal's dimensions are suggested to be 100 meters in width, 2.8 meters in depth, and 6.5 Kilometer in length. Moreover, the suggested Canal (3) should be implemented with the same purpose as canal (2), as this canal is also proposed to be located on the north side.

Canal (3) is expected to lock the floodwater into the city using the maximum inflow quantity as the frequency period of 100 years, which estimated to be almost 1252.6 m^3/s. The direction of this canal starts from the east and extends to the existing bridges over the Jeddah–Jizan Highway; it continues until it reaches the Red sea. The proposed canal's dimension are a width of 150 meters, a depth of 2 meters, and a length of about 7.25 Kilometers. Finally, the recommendations suggest adding Canal (4) on the western side of the Al-Lith valley to adjust and control the floodwater inflow from the north part of the valley. This canal stops the water inflow from penetrating the urban mass using the maximum inflow quantity of the frequency period of 100 years, which is estimated to be almost 599.6 m^3/s. The proposed canal to be instrumented to discharge the water of the valley starts from the east and reaches the sea, with 100 meters as the canal width, 2.8 meters for the depth, and 4 kilometers for the total length.

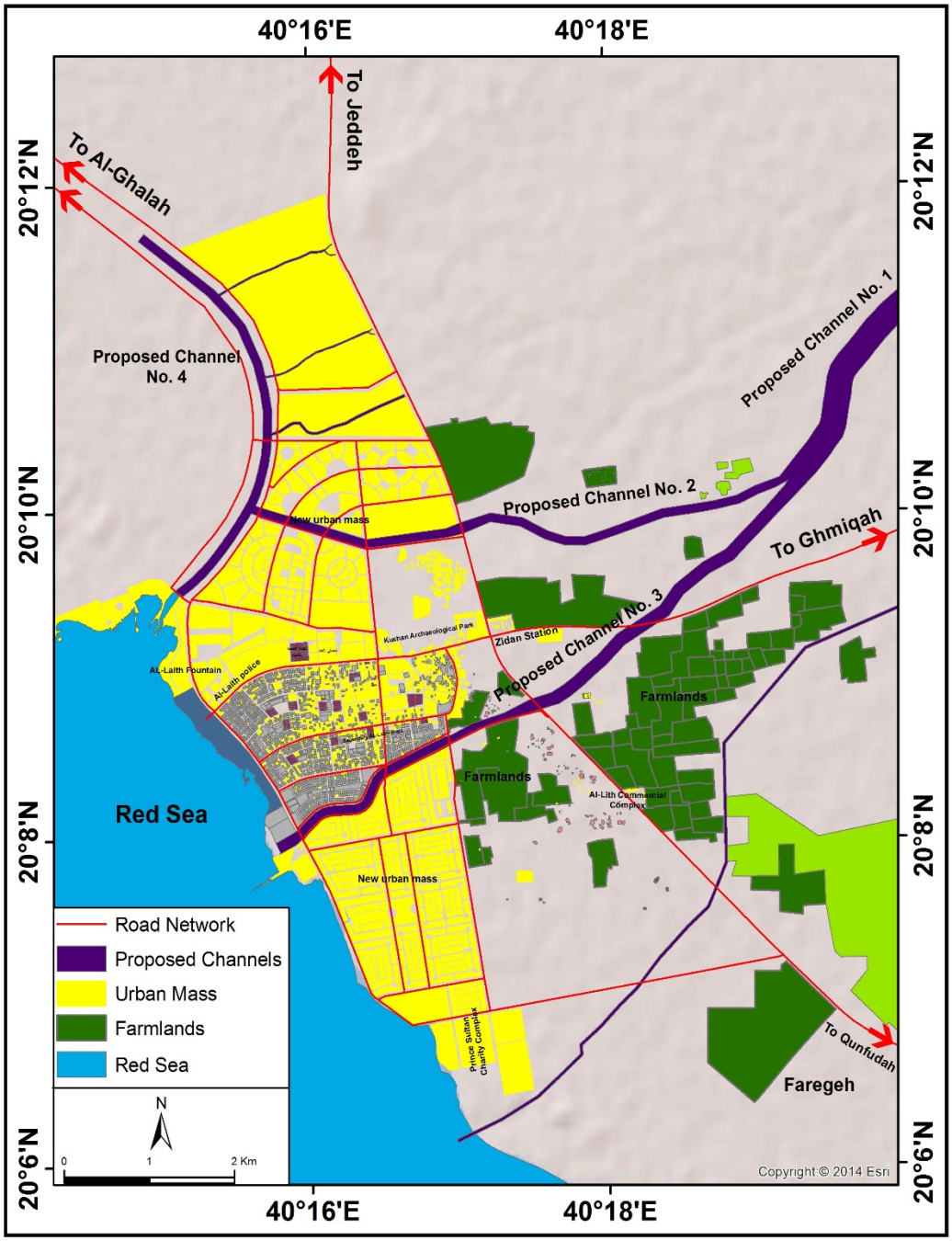

Fig. 22 Map of the alternative suggested protections for preventing flood hazards for Al-Lith city in 2019

The proposals and solutions presented in the manuscript were subjected to public discussion and were discussed with the decision makers at Al-Lith. These discussions were based on the implementation and planning of floods. The quantitative impact of these plans on the ability to reduce flood risk was also measured.

5. RECOMMENDATIONS

The urban environmental management of Saudi cities, as per the Al-Lith city model, requires advanced applied technologies to confront flood hazards. These technologies must be able to determine and test the appropriate variables in the urban growth and change of land use. This will contribute to understanding the nature of floods in environments that experience dynamic changes, since both old maps and traditional instruments are unable to support in developing effective and visibility adapted studies to face flood changes and urban growth. Therefore, this study discusses the implementation of a 2D model that shows the flood water depth, spread, and velocity based on the

hydraulic modelling of the HEC-RAS program for urban developing areas. The study also provides a 2D model of the flood water inflow spread, velocity, and depth, as these characteristics are not available in the one-dimensional flood water inflow model.

The necessity of engineering intervention by implementing 4 Canals, which collects and adjusts the flood water inflow from Al-lith valley basin, This is according to the details of the hydrological and hydraulic characteristics of the proposed mechanism to mitigate the effects of floods on the Al-lith city.

It is important to ensure the continuity of the valleys, determine their campuses, and not block them from any installations or lands that could hinder the movement of torrential water that is suitable for the sea, with the identification of protected areas for the valleys and waterways to maintain them 10 meters from each side in narrow and branched areas and at half the design width of the main valleys. Executive authorities can define this campus and change its width according to the objectives of the plan.

The process of urban expansion of the urban plans from the east of the city of Al-Lith towards the Valley of Al-Lith has been stopped, and no party is allowed to divide, plan, or develop any land or any use of land within the boundaries of urban development or outside it, except with the approval of the land plan by the Ministry of Municipal and Rural Affairs. Thus, approval is necessary for any hydrological studies to ward off the dangers of floods from any project being implemented.

The Council of Ministers Resolution, dated 04/04/1428H, has been implemented. This resolution specifies the controls and procedures that must be taken to counter the damage from torrents and the approval of hydrological studies and engineering designs necessary for the torrents of streams before the approval of residential, agricultural, and other plans, and also not to grant work permits in valleys, except in coordination with the relevant authorities.

The limits of this study do not stop at the conclusions and do not end with the recommendations, as it is possible to take advantage of the spatial database that was created during the completion of this study (as well as its ability to be continuously updated) so the results can be presented to decision-makers to implement them in plans, thereby confronting the risks of torrents and developing and improving the efficiency of the infrastructure for storm water drainage, in line with the Saudi cities future program and the Kingdom's 2030 vision.

6. CONCLUSIONS

Al-Lith city has gone through many challenges over the past 30 years, perhaps the most prominent of which are urban expansions at the expense of natural valleys and increasing environmental changes, as well as a loss of ecological and ecological balance, an increase in groundwater levels, high soil salinity, increased pollution, and exposure to flood risk, all of which require the use of sophisticated modern techniques to determine the negative effects and help mitigate the risk of flooding the city.

The boundaries and paths of the Al-Lith valley near the urban mass of Al-Lith city are unable to be determined using the topographic maps, aerial photographs, and digital elevations. In addition, the difficulty in determining the flood water depth, velocity, and movement of Al-Lith using a one-dimensional model necessitates the creation of a two-dimensional model using the hydraulic modelling program HEC-RAS. Moreover, the admittance of urban schemes and the rapid urban expansion of the city occurred without consideration of the valley's paths, as well as continuous recharges by the residence and service developers. Most of those valleys experience recharge encroachments in the absence of a clear mechanism to protect Al-Lith city from the repeated flood hazard of the Al-Lith valley

Although flood hazard maps can be produced by multiple methods, the basic process is to use the results of an inundation analysis from 1-D or 2-D hydraulic models. A 2-D inundation model is more useful than a 1-D model for creating sophisticated flood hazard maps that are used to forecast flood damage in protected lowlands due to levee failure or overtopping. This is because 2-D models can produce spatially distributed information, including flood depth and velocity across the flooded area.

Using both models (HEC-HMS) and the hydraulic model (HEC-RAS) clarify that the city of Al-Lith is exposed to flood hazards from the main valley extending from east to west (i.e., Al-Lith Valley). The Al-Lith Valley basin was divided into two discharging basins (A, B); the Al-Lith dam, which is used to store water in the valley, was considered in this division. Thus, the flood runoff water from the north side (basin (A)) will be excluded due to the dam reservation of this water volume. The (A) basin extends to 67 kilometers, and its watershed area is about 1890.2 square kilometers, while its basin slope reaches 0.3702 m/m. Basin (B) extends 77 Kilometers, and the total area of the watershed basin is about 1230.6 square kilometers. The slope of the valley basin reaches 0.2118 m/m. The value of water inflow for discharging basins ranges between 1852.52 and 3599.6 m^3/s, the inflow volume is arrayed between 81059586.3 and 127152606.6 m^3, and the period of the inflow ranges between 1080 and 1185 minutes.

This study concludes that dealing with urban

expansion problems, transacting city growth problems, and studying flood hazard prevention before urban planning preparation faces some difficulties in the city, as the relevant knowledge, information, and management expertise were not at a sufficient level to be relied upon to thwart these problems; this field of study also challenges such as the rapid, wide spread, and comprehensive dimensions, and differentiated patterns of urban development. To engage these items with expected flood hazards is a burden for any government or local administration, regardless of its experience and historical success. Therefore, this study helps to clarify the critical points of the continued urban expansion towards valleys, streams, and alluvial fans. It provides a proposal and a vision of the areas suitable for urban development.

According to the development and construction of hydraulic models, the hazard matrix method (the cumulative value between hydraulic and hydrological models with remote sensing techniques) can be used to consider the dynamics of changes in land cover and land use. The urban growth of cities located in the plains and centers of the valleys highlights the need for cities to consider advanced planning for growth in the plains and centers of the valleys in drylands. Therefore, we must determine appropriate paths for the active channels of the floods, and consider stopping encroachments. The paths' dimensions must also be sufficient to discharge the high frequency flood water. This study proposed a mechanism to prevent flood hazards over Al-Lith city; this mechanism is suitable for the city's characteristics and its spatial urban features. This method must be considered and followed in order to develop urban environmental management to alleviate frequent flooding concerns.

7. AUTHOR CONTRIBUTIONS

A.A.K. designed the study, developed the research idea, and planned the research activities. A.A.K., S.S.S.A., H.M.A., and M.M.A. carried out the research, including collecting the input data and preparing the manuscript, and carried out a statistical analysis of the obtained results. A.A.K. carried out a statistical analysis of two-dimensional hydraulic modeling using HEC-RAS, replied to the reviewers' comments, wrote the manuscript, provided valuable comments in writing this paper, professionally edited the manuscript, and designed the methodology. M.M.A. carried out statistical and spatial analyses for monitoring the changes in land use; S.S.S.A. and H.M.A. carried out statistical and spatial analyses for monitoring the changes in the morphology of the valleys in the study area.

8. FUNDING

This research was funded by the Deanship of Scientific Research at Princess Nourah bint Abdulrahman University through the Fast-track Research Funding Program.

9. ACKNOWLEDGMENTS

The authors highly appreciate the great support from the Deanship of Scientific Research at Princess Nourah bint Abdulrahman University through the Fast-track Research Funding Program.

10. CONFLICTS OF INTEREST

The authors declare no conflicts of interest.

11. REFERENCES

[1] Abdel Karim, A., Gaber, A. F. D., Youssef, A. M., and Pradhan, B., Flood Hazard Assessment of the Urban Area of Tabuk City, Kingdom of Saudi Arabia by Integrating Spatial-Based Hydrologic and Hydrodynamic Modeling. MDPI, Sensors, Vol. 19, No. 5, 2019, pp. 1-23.

[2] Dammalage, T. L., and Jayasinghe, N. T., Land-Use Change and Its Impact on Urban Flooding: A Case Study on Colombo District Flood on May 2016, Engineering, Technology & Applied Science Research, Vol. 9, No 2, 2019, pp. 3887-3891.

[3] Manoranjan, M., Monica, R., Gloria, S., Tracy, I., and Paul, L., A Remote Sensing Based Integrated Approach to Quantify the Impact of Fluvial and Pluvial Flooding in an Urban Catchment, MDPI, Remote sensing, Vol. 11, No. 5, 2019, pp. 1-16.

[4] Seid, M., M., Shahram, R., and Hashem, R., Estimation of flood land use/land cover mapping by regional modelling of flood hazard at sub-basin level case study: Marand basin, Geomatics, Natural Hazards and Risk, Vol. 10, Issue 1, 2019, pp. 1155-1175.

[5] Xu, C., Chen, Y., Chen, Y., Zhao, R., and Ding, H., Responses of surface runoff to climate change and human activities in the arid region of Central Asia: A case study in the Tarim River Basin, China. Environ. Manag, Vol. 51, 2013, pp. 926–938.

[6] Poussin, J. K., Botzen, W. J., and Aerts, J. C. J. H. Factors of influence on flood damage mitigation, behavior by households. Environ. Sci. Policy, Vol. 40, 2014, pp. 69–77.

[7] Patel, D. P., Srivastava, P. K., Flood hazards mitigation analysis using remote sensing and GIS: Correspondence with town planning scheme. Water Resour. Manag, Vol. 27, Issue 7, 2013, pp. 2353–2368.

[8] Moel, H. D., Vliet, M. V., and Aerts, J. C. J. H., Evaluating the effect of flood damage-reducing measures: A case study of the unembanked area of Rotterdam, the Netherlands. Reg. Environ. Change, Vol. 14, Issue 3, 2014, pp. 895–908.
[9] Althuwaynee, O. F., Pradhan, B., Park, H-J., and Lee, J. H., A novel ensemble bivariate statistical evidential belief function with knowledge-based analytical hierarchy process and multivariate statistical logistic regression for landslide susceptibility mapping. Catena, Vol. 114, 2014, pp. 21–36.
[10] Van Westen, C. J., Rengers, N., and Soeters, R., Use of geomorphological information in indirect landslide susceptibility assessment. Nat. Hazards, Vol. 30, Issue, 3, 2003, pp. 399–419.
[11] Lee, M. J., Kang, J. E., and Jeon, S., Application of frequency ratio model and validation for predictive flooded area susceptibility mapping using GIS. In Proceedings of the Geoscience and Remote Sensing Symposium (IGARSS), Munich, Germany, 2012, pp. 895–898.
[12] Tehrany, M. S., Pradhan, B., Mansor, S., and Ahmad, N., Flood susceptibility assessment using GIS-based support vector machine model with different kernel types. Catena, Vol. 125, 2015, pp. 91–101.
[13] Stefanidis, S., and Stathis, D., Assessment of flood hazard based on natural and anthropogenic factors using analytic hierarchy process (AHP). Nat. Hazards, Vol. 68, 2013, pp. 569–585.
[14] Pradhan, B., Use of GIS-based fuzzy logic relations and its cross application to produce landslide susceptibility maps in three test areas in Malaysia. Environ. Earth Sci, Vol. 63, 2011, pp. 329–349.
[15] Pradhan, B., Flood susceptible mapping and risk area delineation using logistic regression, GIS and remote sensing. J. Spat. Hydrol, Vol. 9, No. 2, 2010, pp. 1–18.
[16] Samanta, S., Pal, D. K., Lohar, D., and Pal, B., Interpolation of climate variables and temperature modeling. Theor. Appl. Climatol, Vol. 107, 2012, pp. 35–45.
[17] Kia, M. B., Pirasteh, S., Pradhan, B., Mahmud, A. R., Sulaiman, W. N. A., and Moradi, A., An artificial neural network model for flood simulation using GIS: Johor River Basin, Malaysia. Environ. Earth Sci, Vol. 67, Issue 1, 2012, pp. 251–264.
[18] Lohani, A. K., Goel, N. K., and Bhatia, K. K. S., Improving real time flood forecasting using fuzzy inference system. J. Hydrol, Vol. 509, 2014, pp. 25–41.
[19] Tehrany, M. S., Pradhan, B., and Jebur, M. N., Flood susceptibility mapping using a novel ensemble weights-of-evidence and support vector machine models in GIS. J. Hydrol, Vol. 512, 2014, pp. 332–343.
[20] Koloa, C. M., and Samanta, S., Development Impact Assessment Along Merkham River through Remote Sensing and GIS Technology. Int. J. Asian Acad. Res. Ass, 5, 2013, pp. 26–41.
[21] Malczewski, J., GIS-based multicriteria decision analysis: A survey of the literature. Int. J. Geogr. Inf. Sc, Vol. 20, Issue 7, 2006, pp. 703–726.
[22] Jia, Y., and Wang, S., CCHE2D: Two-Dimensional Hydrodynamic and Sediment Transport Model for Unsteady Open Channel Flows over Loose Bed; National Center of Computational Hydroscience and Engineering: Nutrioso, AZ, USA, 2001.
[23] O'Brien, S., FLO-2D: Two-Dimensional Flood Routing Mode; FLO-2D Software, 2017, Available online: https://www.flo-2d.com/wp-content/uploads/2018/09/FLO-2D-Plugin-Users-Manual.pdf (accessed on 12 April 2018).
[24] Deltares. SOBEK: Hydrodynamics, Rainfall and Real-Time Control User Manual; Deltares: Delft, The Netherlands, 2019, pp. 1-932.
[25] Danish Hydraulic Institute., MIKE-Flood User Manual; Danish Hydraulic Institute: Horsholm, Denmark, 2017, pp. 1-152.
[26] Bradbrook, K., JFLOW: A multiscale two-dimensional dynamic flood model. J. Water Environ. Technol, Vol. 2, 2007, pp. 79–86.
[27] Bates, P., Trigg, M., Neal, J., and Dabrowa, A., LISFLOOD-FP User Manual; University of Bristol: Bristol, UK, 2013.
[28] Meghan, A., Christophe, V., hazel, F., and Sally, Priest., flood risk management Consortium Methods for creating a flood Risk Assessment tool, Flood hazard Research center, 2011, pp. 6-58.
[29] Mohamed, A., Amro, E., Ahmed, K., Moustafa, K., Nassir, A., Anis, C., and Kashif, N., Flash flood risk assessment in urban arid environment: case study of Taibah and Islamic universities' campuses, Medina, Kingdom of Saudi Arabia. Geomatics, Natural Hazards and Risk, Vol. 10, Issue 1, 2019, pp. 780-796.
[30] Hatim, S., Farhan, A., Abdulaziz, A., Ibrahim, A., Eyad, F., Salem, J., and Almoutaz, E., Flood hazards in an urbanizing watershed in Riyadh, Saudi Arabia. Geomatics. Natural Hazards and Risk, Vol. 7, Issue 2, 2016, pp. 702-720.
[31] Abdelkarim, A., Gaber, D., Alkadi, I., and Alogayell, M., Integrating Remote Sensing and Hydrologic Modeling to Assess the Impact of Land-Use Changes on the Increase of Flood Risk: A Case Study of the Riyadh–Dammam Train Track, Saudi Arabia, MDPI, Sustainability, Vol. 11, No. 21, 2019, pp. 1-32.
[32] Muhammad A., Ahmed, A., and Hatim, O., Estimating urban flooding potential near the

outlet of an arid catchment in Saudi Arabia. Geomatics. Natural Hazards and Risk, Vol. 8, Issue 2, 2017, pp. 672–688.

[33] Norhan, A., Saud, T., Fahad, A., and Kamarul, A. Arid hydrological modeling at wadi Alaqiq, Madinah, Saudi Arabia. Jurnal Teknologi, Vol. 78, No. 7, 2016, pp. 51–58.

[34] Sampath, D., Weerakoon, S., and Herath, S., HEC-HMS model for runoff simulation in a tropical catchment with intra-basin diversions case study of the Deduru Oya River Basin, Sri Lanka. Engineer, Vol. 48, No. 1, 2015, pp. 1-9.

[35] Meiling, W., Lei Z., and Thelma, D., Hydrological modeling in a semi-arid region using HEC-HMS. Journal of Water Resources and Hydraulic Engineering, Vol. 5, Issue, 3, 2016, pp. 105-115.

[36] Laouacheria, F., and Mansouri, R., Comparison of WBNM and HEC-HMS for runoff hydrograph prediction in a small urban catchment. Water Resources Management, Vol. 29, 2015, pp. 2485–2501.

[37] Khalil, R., Khaled, B., and Amjad, M., Sub-catchments flow losses computation using Muskingum–Cunge routing method and HEC-HMS GIS based techniques, case study of Wadi Al -Lith, Saudi Arabia. Model. Earth Syst. Environ, Vol. 92, 2017, pp. 1027-1049.

[38] Alin, M. P., Catalin, I. C., Cristian, C. S., Martín, N. P., and Larisa, E. P., Using High-Density LiDAR Data and 2D Streamflow Hydraulic Modeling to Improve Urban Flood Hazard Maps: A HEC-RAS Multi-Scenario Approach. MDPI, Water, 11(9), 2019, pp. 1-24.

[39] Keisuke, Y., Shiro, M., Shuhei, O., Koji, M., and Shinya, N. Estimation of distributed flow resistance in vegetated rivers using airborne topo-bathymetric LiDAR and its application to risk management tasks for Asahi River flooding. Journal of Flood Risk Management, 2019, pp. 1-17.

[40] Talisay, B. A. M., Puno, G. R., and Amper, R. A. L., Flood hazard mapping in an urban area using combined hydrologic-hydraulic models and geospatial technologies. Global Journal of Environmental Science and Management (GJESM), Vol. 5, No. 2, 2019, pp. 139-154.

[41] Congalton, R. G.; A review of assessing the accuracy of classifications of remotely sensed data, Remote Sensing of Environment, Vol. 37, Issue 1, 1991, pp. 35-46.

[42] Ponce, V. M., and Hawkins, R. H., Runoff Curve Number: Has It Reached Maturity?. Journal of Hyrologic Engineering, Vol. 1, Issue 1, 1996, pp. 9-20.

[43] US Army Corps of Engineers (USACE). Hydrologic Modeling System HEC-HMS Technical Reference Manual; Hydrologic Engineering Center: Davis, CA, USA, 2000.

[44] Fan, C.; Ko, C. H., and Wang, W. S., An innovative modeling approach using Qual2K and HEC-RAS integration to assess the impact of tidal effect on River Water quality simulation. J. Environ Manag, Vol. 90, Issue 5, 2009, pp. 1824–1832.

[45] Anderson, M. L., Chen, Z. Q.; Kavvas, M. L., and Feldman, A., Coupling HEC-HMS with atmospheric models for prediction of watershed runoff. J. Hydrol Eng, Vol. 7, Issue 4, 2002, pp. 312–318.

[46] Siddiqui, Q. T. M., Hashmi, H. N., Ghumman, A. R., and Mughal, H. U. R., Flood inundation modeling for a watershed in the pothowar region of Pakistan. Arab. J. Sci Eng, Vol. 36. 2011, pp. 1203–1220.

[47] Hyfran, M. Developed by INRS-Eau with Collaboration of Hydro-Québec Hydraulic Service (Department Hydrology). in the Framework of Hydro-Québec/CRSNG Statistical Hydrology Chair Located at INRS-Eau, 1998.

[48] Soil Conservation Services, (SCS), National Engineering Handbook. Section 4: Hydrology. US Department of Agriculture. Soil Conservation Service. Engineering Division. Washington DC. 1985.

[49] Istomina, M. N., Kocharyan, A. G., and Lebedeva, I. P., Floods: Genesis, socioeconomic and environmental impacts. Water Resour, Vol. 32, 2005, pp. 349–358.

[50] Brath, A., Montanari, A., and Moretti, G., Assessing the effect on flood frequency of land use change via hydrological simulation (with uncertainty). J. Hydrol, Vol. 342, Issue 1-4, 2006, pp. 141–153.

[51] Mao, D., and Cherkauer, K. A., Impacts of land-use change on hydrologic responses in the Great Lakes region. J. Hydrol. Vol. 374, Issue 1-2, 2009, pp. 71–82.

[52] Sheng, J., and Wilson, J. P., Watershed urbanization and changing flood behavior across the Los Angeles metropolitan region. Nat. Hazards, Vol. 48, 2009, pp. 41–57.

[53] Solin, L., Feranec, J., and Novacek, J., Land cover changes in small catchments in Slovakia during 1990-2006 and their effects on frequency of flood events. Nat. Hazards, Vol. 56, 2011, pp. 195–214.

[54] Nirupama, N., and Simonovic, S. P., Increase of flood risk because of urbanization: A Canadian example. Nat. Hazards, Vol. 40, 2007, pp. 25–41.

[55] Saghafian, B., Farazjoo, H., Bozorgy, B., and Yazdandoost, F., Flood intensification because of changes in land use. Water Resour. Manag, Vol. 22, 2008, pp. 1051–1067.

[56] Suarez, P., Anderson, W., Mahal, V., and Lakshmanan, T. R., Impacts of flooding and

climate change on urban transportation: A system wide performance assessment of the Boston Metro Area. Transp. Res, Vol. 10, Issue 3, 2005, pp. 231–244.
[57] Ramachandra, T. V., and Mujumdar, P. P., Urban floods: Case study of Bangalore. Disaster Dev, Vol. 3, 2009, pp. 1–98.
[58] Huong, H. T. L., and Pathirana, A. Urbanization and climate change impacts on future urban flooding in Can Tho city, Vietnam. Hydrol. Earth Syst. Sci, Vol. 17, Issue 1, 2013, pp. 379–394.
[59] Neuvel, J. M. M., and van den Brink, A. Flood risk management in Dutch local spatial planning practices. J. Environ. Plan. Manag, Vol. 52, Issue, 7, 2009, pp. 865–880.
[60] Audisio, C., and Turconi, L., Urban floods: A case study in the Savigliano area (North-Western Italy). Nat. Hazards Earth Syst. Sci, Vol. 11, Issue 11, 2011, pp. 2951–2964.
[61] Špitalar, M., Gourley, J. J., Lutoff, C., Kirstetter, P. E., Brilly, M., and Carr, N., Analysis of flash flood parameters and human impacts in the US from 2006 to 2012. J. Hydrol, Vol. 519, Part A, 2014, pp. 863–870.
[62] Ran, J., and Nedovic-Budic, Z., Integrating spatial planning and flood risk management: A new conceptual framework for the spatially integrated policy infrastructure. Comput. Environ. Urban Syst, Vol. 57, 2016, pp. 68–79.
[63] Sanyal, J., Lu, X. X. Application of remote sensing in flood management with special reference to monsoon Asia: A review. Nat. Hazards, Vol. 33, 2004, pp. 283–301.
[64] Dewan, A. M., Islam, M. M., Kumamoto, T., and Nishigaki, M. Evaluating flood hazard for land-use planning in Greater Dhaka of Bangladesh using remote sensing and GIS techniques. Water Resour. Manag, Vol. 21, 2007, pp. 1601–1612.
[65] Kadiogullari, A. I., and Baskent, E. Z., Spatial and temporal dynamics of land use pattern in Eastern Turkey: A case study in Gumushane. Environ. Monit. Assess, Vol. 138, 2008, pp. 289–303.
[66] Chen, J., Hill, A. A., Urbano, L. D., A GIS-based model for urban flood inundation. J. Hydrol, Vol. 373, Issue 1-2, 2009, pp. 184–192.
[67] Mishra, A. K., study on the occurrence of flood events over Jammu and Kashmir during September 2014 using satellite remote sensing. Nat. Hazards, Vol. 78, 2015, pp. 1463–1467.